

A Track-Before-Detect Trajectory Multi-Bernoulli Filter for Generalised Superpositional Measurements

Sion Lynch, Ángel F. García-Fernández and Lee Devlin

Abstract—This paper proposes the Trajectory-Information Exchange Multi-Bernoulli (T-IEMB) filter to estimate sets of alive and all trajectories in track-before-detect applications with generalised superpositional measurements. This measurement model has superpositional hidden variables which are mapped to the conditional mean and covariance of the measurement, enabling it to describe a broad range of measurement models. This paper also presents a Gaussian implementation of the T-IEMB filter, which performs the update by approximating the conditional moments of the measurement model, and admits a computationally light filtering solution. Simulation results for a non-Gaussian radar-based tracking scenario demonstrate the performance of two Gaussian T-IEMB implementations, which provide improved tracking performance compared to a state-of-the-art particle filter based solution for track-before-detect, at a reduced computational cost.

Index Terms—Multi-target tracking, sets of trajectories, track-before-detect, superpositional measurements, multi-Bernoulli.

I. INTRODUCTION

Target tracking involves estimating the evolution of an object’s state using sensor information corrupted by noise [1]. Common applications of target tracking include radar-based surveillance [2], autonomous surface vehicles [3], and space surveillance [4]. Typical target tracking schemes use point detections, which are extracted from raw sensor measurements using a thresholding scheme, and subsequently used to perform tracking. Track-before-detect (TkBD) [5]–[10] is an alternative approach in which sensor measurements forego any processing or thresholding, such that raw sensor measurements are used to perform tracking. This is advantageous when tracking targets with a weak return signal, as they are unlikely to produce a detection using traditional processing or thresholding schemes.

Early approaches for TkBD typically assume there is at most a single target present [11] [12]. A natural approach to tackle TkBD problems with an unknown and time-varying number of targets is to use the Random Finite Set (RFS) [13] framework. RFS-based filters model the multi-target state of interest as a set, which captures uncertainty on both the number and states of the targets. The RFS framework therefore provides a unified theoretical framework for handling target birth, death and updating existing state estimates.

This work was jointly supported by the University of Liverpool and Leonardo UK.

Sion Lynch and Lee Devlin are with the Department of Electrical Engineering and Electronics, University of Liverpool, L69 3GJ U.K. (emails: {sion.lynch, l.devlin}@liverpool.ac.uk).

Ángel García-Fernández is with Information Processing and Telecommunications Center, ETSI de Telecomunicación, Universidad Politécnica de Madrid, 28040 Madrid, Spain (email: angel.garcia.fernandez@upm.es).

Derivations of RFS-based filters for TkBD require a suitable choice of measurement model, which characterises the probability distribution of the received signal depending on the number of targets and their states. To model general TkBD sensors, one can use a general measurement model, as in [14]–[16], which typically requires the use of particle filters to perform the inference task. Some techniques are then usually necessary to address the curse of dimensionality [17].

Alternatively, the measurement model of the sensing system may be superpositional [13, Chapter 19]. In this model, the measurement, typically its conditional mean given the multi-target state, is dependent on the summation, or superposition, of multiple target contributions. Superpositional measurements typically model the received signal at a sensor, such as an acoustic [18] or active/passive radio-frequency sensor [19], where the received signal originates from multiple signal emitters and additive noise, typically Gaussian [20]. This superpositional property enables the development of a variety of TkBD filters. For instance, a Probability Hypothesis Density (PHD) filter and Cardinalised PHD filter for superpositional measurements have been proposed, using a Sequential Monte Carlo (SMC) i.e. particle filter [18], or Gaussian mixture [21] implementation. Multi-Bernoulli (MB) filters have also been extended to superpositional measurements [22], with an SMC implementation proposed in [23].

The Information Exchange Multi-Bernoulli (IEMB) filter [5] is a TkBD filter for superpositional measurements that propagates an MB density for the set of targets. The updated MB density minimises the Kullback-Leibler divergence (KLD) [24] between the exact updated density and its MB approximation, when the target states are augmented with auxiliary variables. The IEMB filter runs a Bernoulli filter for each potential target independently, with an exchange of information among filters to account for the effect of other potential targets on the mean and covariance matrix of the measurement. This approach bears similarity to the multiple filtering technique for a fixed and known number of targets. This technique, used for particle filtering [20] [25] and Gaussian filtering [26], applies a separate filter to each target accounting for the mean of the other targets (and possibly the covariance) in the measurement model.

Standard approaches to TkBD, such as all those mentioned so far, produce an approximation to the posterior density of the set of targets. This density provides information only on the current state of each target. In many applications full target tracks or trajectories are of interest, as they provide more information on target nature or behaviour. Trajectories can be formed using a track building scheme, which sequentially

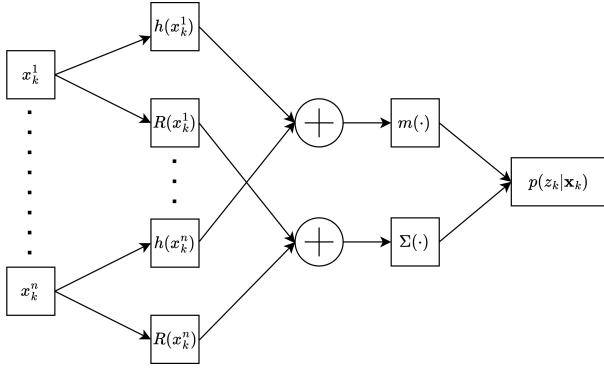


Figure 1: Graphical representation of how n targets $\mathbf{x}_k = \{x_k^1, \dots, x_k^n\}$ at time step k contribute to the measurement through each hidden measurement function $h(\cdot)$ and covariance function $R(\cdot)$, which are summed over all targets and passed through the mapping functions $m(\cdot)$ and $\Sigma(\cdot)$, providing the conditional mean and covariance of the measurement.

links labelled state estimates into a full target track [13]. Alternatively, trajectories can be estimated from first principles by developing filters which directly estimate target trajectories, known as trajectory based multi target-tracking filters [27]–[30]. Such filters then produce posterior densities over the set of target trajectories, rather than only the current set of targets, and provide a fully Bayesian approach for estimating multiple target trajectories.

In this paper, we present a TkBD multi-target tracking filter based on sets of trajectories with generalised superpositional measurements. The first contribution of this paper is the definition of this type of measurement model. This model is characterised by the conditional mean and covariance of the measurement given the set of targets, as these moments are required to develop Gaussian filters [31]. Its main characteristic is that to obtain these moments, the target states are first projected non-linearly to certain hidden features. The obtained features for the mean and covariance matrix have the superpositional property and therefore summed over the targets. Finally, non-linear mappings are applied to both the conditional mean and covariance. A graphical representation of this measurement model is provided in Figure 1. This model is important as it allows us to address a wider range of superpositional measurements, for example Rician distributed TkBD measurements in ground radar-based surveillance [32, Chapter 8], or K-distributed TkBD measurements found in maritime radar-based surveillance [33]. The second contribution is an approximate form of the conditional mean and covariance of the generalised superpositional measurements given the set of targets. The conditional moments are then used to perform a Gaussian update of the single-target densities at each time step [31].

The third contribution of this paper is to extend the IEMB to estimate sets of trajectories, giving rise to the Trajectory-IEMB filter (T-IEMB). The T-IEMB filter propagates a Trajectory MB (TMB) density for the set of trajectories, and also uses a KLD minimisation approach to derive an approximate updated TMB density, as illustrated in Figure 2. The T-IEMB filters that obtain the information on the set of alive trajectories and the

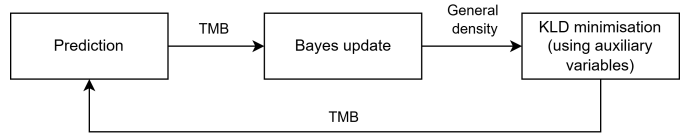


Figure 2: T-IEMB filter diagram. A Bayes update of the predicted TMB density and considered likelihood yields a general non-TMB density. An approximate updated TMB density is derived by minimising the KLD (after the introduction of the auxiliary variables) [5].

set of all trajectories are derived. We also propose a Gaussian implementation for the generalised superpositional measurement model. This is performed using analytical linearisation of the external functions that provide the conditional mean and covariance matrix, and the application of the Iterated Posterior Linearisation Filter (IPLF) [31] [34]. The resulting T-IEMB filters provide a computationally light filtering solution, which directly estimates trajectories from generalised superpositional measurements. A preliminary version of this work is [35], which presented the T-IEMB filter for alive trajectories and Gaussian superpositional measurements.

The remainder of this paper is organised as follows. Section II details the models used and problem formulation. Section III presents the T-IEMB filtering recursion for alive and all trajectories. Section IV presents the update stage of the Gaussian implementation of the T-IEMB. Section V presents simulation results, and Section VI discusses conclusions of the work.

II. MODELS AND PROBLEM FORMULATION

This paper aims to solve two multi-target tracking problems in TkBD scenarios with a generalised superpositional measurement model: estimating the set of alive trajectories at the current time step, and estimating the set of all trajectories up to the current time step [29]. To achieve this, in this section we firstly present the multi-target dynamic model in Section II-A, the generalised superpositional measurement model in Section II-B, and sets of trajectories in Section II-C.

A. Multi-Target Dynamic Model

We consider a standard multi-target state and model. An individual target state $x_k \in \mathbb{R}^{n_x}$, where n_x is the dimensionality of x_k , belongs to the set of targets \mathbf{x}_k at time step k , such that $\mathbf{x}_k \in \mathcal{F}(\mathbb{R}^{n_x})$, where $\mathcal{F}(\mathbb{R}^{n_x})$ denotes the set of all finite subsets of \mathbb{R}^{n_x} . A target with state x_k moves within the surveillance area, surviving to the next time step with a probability of survival $p^S(x_k)$, with transition density $g(\cdot|x_k)$. The multi-target state \mathbf{x}_k consists of both surviving targets and new targets.

New targets are born according to an MB birth model consisting of n_k^b birth components, with MB density [28]

$$f_k^b(\mathbf{x}_k) = \sum_{\mathbf{x}^1 \uplus \dots \uplus \mathbf{x}^{n_k^b} = \mathbf{x}_k} \prod_{l=1}^{n_k^b} f_k^{b,l}(\mathbf{x}^l) \quad (1)$$

where \uplus denotes disjoint union, and the summation sums over all disjoint and possibly empty subsets $\mathbf{x}^1, \dots, \mathbf{x}^{n_k^b}$ such that

their union is \mathbf{x}_k , which is a result of the convolution sum for independent RFSs [13]. The l th Bernoulli birth component has a density

$$f_k^{b,l}(\mathbf{x}_k) = \begin{cases} 1 - p_b^l & \mathbf{x}_k = \emptyset \\ p_b^l b_k^l(x) & \mathbf{x}_k = \{x\} \\ 0 & \text{otherwise} \end{cases} \quad (2)$$

where \emptyset is the empty set, p_b^l is the birth probability, and $b_k^l(\cdot)$ is the single-target birth density.

B. Generalised Superpositional Measurement Model

Targets are observed using a sensor system comprising of M sensors, with the j th sensor generating a measurement $z_k^j \in \mathbb{R}^{n_z}$, where $j \in \{1, \dots, M\}$. The measurement from each sensor can be combined into a measurement vector $z_k = [(z_k^1)^T, \dots, (z_k^M)^T]^T$, where $(\cdot)^T$ denotes matrix transpose. In this paper, we use a generalised superpositional measurement model, which we proceed to detail.

The sensor model has a nested architecture. Firstly, there is an internal measurement function $h(\cdot)$ and internal covariance function $R(\cdot)$, which consider all sensors at once as

$$h(x_k) = [h^1(x_k), \dots, h^M(x_k)]^T \quad (3)$$

$$R(x_k) = \text{diag}(R^1(x_k), \dots, R^M(x_k)) \quad (4)$$

where $\text{diag}(\cdot)$ denotes a block-diagonal matrix with the indicated matrices across the diagonal. Then, the conditional mean and covariance matrix of the measurement can be written as

$$\mathbb{E}[z_k | \mathbf{x}_k] = m \left(\sum_{x_k \in \mathbf{x}_k} h(x_k) \right) \quad (5)$$

$$\mathbb{C}[z_k | \mathbf{x}_k] = \Sigma \left(\sum_{x_k \in \mathbf{x}_k} R(x_k) \right) \quad (6)$$

where $m(\cdot)$ is a function that maps the sum of internal measurements to a vector of size $Mn_z \times 1$, and $\Sigma(\cdot)$ is a function that maps the sum of internal covariance matrices to a covariance matrix of dimensions $Mn_z \times Mn_z$. We then assume the conditional moments (5) and (6) are sufficient statistics of the conditional density of the measurement given the set of targets, such that we can write

$$p(z_k | \mathbf{x}_k) = l(z_k | \mathbb{E}[z_k | \mathbf{x}_k], \mathbb{C}[z_k | \mathbf{x}_k]). \quad (7)$$

We proceed to explain this measurement model using an example, and was graphically illustrated in Figure 1.

Example 1. If the measurement $z_k \in \mathbb{R}$ is the received pulse amplitude from a Swerling 1 target in a radar system, whose Radar Cross Section (RCS) is modelled as a random variable, the density of the measurement is Rayleigh distributed as [36, Chapter 7]

$$p(z_k | \mathbf{x}_k) = \frac{2z_k}{\sum_{x_k \in \mathbf{x}_k} h(x_k)} \exp \left(-\frac{(z_k)^2}{\sum_{x_k \in \mathbf{x}_k} h(x_k)} \right) \quad (8)$$

where $\sum_{x_k \in \mathbf{x}_k} h(x_k)$ gives the mean RCS of all targets illuminated by the radar, and is 0 otherwise. Using the known results for the mean and variance of the Rayleigh distribution

[37], we can write the mean and covariance mapping functions (5) and (6) for the measurement vector as

$$\mathbb{E}[z_k | \mathbf{x}_k] = m \left(\sum_{x_k \in \mathbf{x}_k} h(x_k) \right) = \sqrt{\frac{\pi}{4}} \sum_{x_k \in \mathbf{x}_k} h(x_k) \quad (9)$$

$$\mathbb{C}[z_k | \mathbf{x}_k] = \Sigma \left(\sum_{x_k \in \mathbf{x}_k} R(x_k) \right) = \frac{4 - \pi}{4} \sum_{x_k \in \mathbf{x}_k} h(x_k) \quad (10)$$

where in this case $\sum_{x_k \in \mathbf{x}_k} R(x_k) = \sum_{x_k \in \mathbf{x}_k} h(x_k)$ (since the Rayleigh distribution is parameterised by a single parameter). Another example is the Rice distribution, which will be considered for the simulations in Section V.

Note that this measurement model is not a standard superpositional model, which would require $m(\cdot)$ to be the identity function, and $\Sigma(\cdot)$ to map to a constant covariance matrix [13].

C. Sets of Trajectories

In this paper we aim to infer sets of trajectories, arising from the multi-target model in Section II-A, and from measurements distributed according to the model in Section II-B. We consider the single-trajectory variable $X = (t, x^{1:v})$, where t is the time step at which the trajectory began, and $x^{1:v} = (x^1, \dots, x^v)$ is the sequence of target states of length v . The start time and length (t, v) therefore belong to the set $I_{(k)} = \{(t, v) : 0 \leq t \leq k \text{ and } 1 \leq v \leq k-t+1\}$, and the single-trajectory space up to the current time step k is then $T_{(k)} = \uplus_{(t,v) \in I_{(k)}} \{t\} \times \mathbb{R}^{vn_x}$ [27]. A set of trajectories up to the current time step k is denoted by \mathbf{X}_k , where the set of trajectories $\mathbf{X}_k \in \mathcal{F}(T_{(k)})$.

We use $\tau^k(X)$ to denote the single-target at time step k corresponding to trajectory X . This set may be empty or contain one element with the expression

$$\tau^k(t, x^{1:v}) = \begin{cases} \{x^{k-t+1}\} & t \leq k \leq t+v-1 \\ \emptyset & \text{elsewhere.} \end{cases} \quad (11)$$

Similarly, \mathbf{x}_k denotes the set of targets at time step k corresponding to the set of trajectories \mathbf{X}_k . Integration over sets of trajectories is reviewed in Appendix A.

In a Bayesian framework, all information about the set of considered trajectories (either the alive or all trajectories [29]) is included in its posterior density, which can be written in terms of the prediction and update steps [27]. Since the update step is intractable for the measurement model (7), we propose an approximate TMB filter in the next section.

III. TRAJECTORY IEMB FILTER

In this section we begin by detailing the dynamic model for the set of alive and all trajectories in Section III-A, before presenting the TMB density in Section III-B, which is propagated through the T-IEMB prediction and update recursions in Section III-C and III-D, respectively.

A. Dynamic Models for Sets of Trajectories

Sets of alive and all trajectories evolve according to the following dynamic models, which are derived from the dynamic model for the sets of targets [28]. Following (1), new

trajectories are born at time step k according to an MB birth model for trajectories

$$f_k^b(\mathbf{X}_k) = \sum_{\mathbf{X}^1 \cup \dots \cup \mathbf{X}^{n_k^b} = \mathbf{X}_k} \prod_{l=1}^{n_k^b} f_k^{b,l}(\mathbf{X}^l) \quad (12)$$

where each Bernoulli component is now a trajectory of length 1 born at time step k

$$f_k^{b,l}(\mathbf{X}_k) = \begin{cases} 1 - p_b^l & \mathbf{X}_k = \emptyset \\ p_b^l b_k^l(x) & \mathbf{X}_k = \{(k, x)\} \\ 0 & \text{otherwise.} \end{cases} \quad (13)$$

Note that this density corresponds to the birth model for sets of targets, adding the time index k to the state. A trajectory X survives to the next time step with probability $p^S(X)$ and evolves with a single-trajectory density $g_{k+1}(\cdot | X)$. The single-trajectory dynamic model differs if we consider alive or all trajectories.

1) *Dynamic Model for Sets of Alive Trajectories*: When estimating the set of alive trajectories, the filtering density at any time step contains information on only the trajectories that are alive. At any time step k , each alive trajectory $X = (t, x^{1:v})$ in the set of alive trajectories \mathbf{X}_k , survives to the next time step with probability $p^S(X) = p^S(x^v)$, and evolves according to the single-trajectory transition density [29]

$$g_{k+1}(t_y, y^{1:v_y} | X) = \delta_t[t_y] \delta_{v+1}[v_y] \delta_{x^{1:v}}(y^{1:v_y-1}) \times g(y^{v_y} | x^v) \quad (14)$$

where the Kronecker delta $\delta_t[t_y] = 1$ if $t = t_y$, and $\delta_{x^{1:v}}(y^{1:v_y-1})$ is the Dirac delta located at $x^{1:v}$ and evaluated at $y^{1:v_y-1}$. Trajectories alternatively die with probability $1 - p^S(x^v)$.

The set of alive trajectories at time step $k+1$ is then the union of surviving trajectories, which have evolved according to (14), and new trajectories which have been born according to the MB birth model (13).

2) *Dynamic Model for Sets of All Trajectories*: The filtering density for sets of all trajectories contains both alive trajectories, and trajectories which have died at a previous time step and are no longer evolving. Therefore, at any time step k , each trajectory $X = (t, x^{1:v})$ in the set of all trajectories \mathbf{X}_k survives to the next time step with probability $p^S(X) = 1$, with single-trajectory transition density [29]

$$g_{k+1}(t_y, y^{1:v_y} | X) = \delta_t[t_y] \times \begin{cases} \delta_v[v_y] \delta_{x^{1:v}}(y^{1:v_y}) & \omega_y < k \\ \delta_v[v_y] \delta_{x^{1:v}}(y^{1:v_y})(1 - p^S(x^v)) & \omega_y = k \\ \delta_{v+1}[v_y] \delta_{x^{1:v}}(y^{1:v_y-1}) p^S(x^v) \\ \times g(y^{v_y} | x^v) & \omega_y = k+1 \end{cases} \quad (15)$$

where $\omega_y = t_y + v_y - 1$. That is, each trajectory stays in the set of trajectories with probability 1, and its length increases with probability $p^S(x^v)$. New trajectories are born according to the same MB birth model (13) as for the set of alive trajectories.

B. Trajectory Multi-Bernoulli Density

The proposed TkBD filter propagates MB densities on the set of trajectories through the filtering recursion. That is, the predicted and posterior densities at time step k given the measurements up to time step $k' \in \{k, k-1\}$ are TMB of the form [28]

$$f_{k|k'}(\mathbf{X}_k) = \sum_{\bigcup_{l=1}^{n_{k|k'}} \mathbf{X}^l = \mathbf{X}_k} \prod_{i=1}^{n_{k|k'}} f_{k|k'}^i(\mathbf{X}^i) \quad (16)$$

where $n_{k|k'}$ is the number of Bernoulli components, and

$$f_{k|k'}^i(\mathbf{X}_k) = \begin{cases} 1 - r_{k|k'}^i & \mathbf{X}_k = \emptyset \\ r_{k|k'}^i p_{k|k'}^i(X) & \mathbf{X}_k = \{X\} \\ 0 & \text{otherwise} \end{cases} \quad (17)$$

where $r_{k|k'}^i$ is the probability of existence of the i th Bernoulli component, and $p_{k|k'}^i(X)$ is the single-trajectory density, which has a deterministic known start time t^i .

C. T-IEMB Filter Prediction

The T-IEMB filter prediction is equivalent to the TMB filter prediction [28], since the dynamic models are the same.

Lemma 2 (T-IEMB Prediction). *Given a TMB posterior of the form (16), the predicted density is TMB of the form (16) with $n_{k|k-1} = n_{k-1|k-1} + n_k^b$ components, where the probability of existence and single-trajectory density of each $i \in \{1, \dots, n_{k-1|k-1}\}$ Bernoulli is [28]*

$$r_{k|k-1}^i = r_{k-1|k-1}^i \int p^S(X') p_{k-1|k-1}^i(X') dX' \quad (18)$$

$$p_{k|k-1}^i(X) = \frac{\int g_k(X | X') p^S(X') p_{k-1|k-1}^i(X') dX'}{\int p^S(X') p_{k-1|k-1}^i(X') dX'} \quad (19)$$

where the integral is a single-trajectory integral (see Appendix A), $g_k(X | X')$ is the transition density (14) for alive trajectories, and (15) for all trajectories. For each $i \in \{n_{k-1|k-1} + 1, \dots, n_{k-1|k-1} + n_k^b\}$, its Bernoulli birth component is

$$f_{k|k-1}^i(\mathbf{X}) = f_k^{b,i-n_{k-1|k-1}}(\mathbf{X}). \quad (20)$$

D. T-IEMB Filter Update

To present the T-IEMB filter update, we first present a more explicit form of the single-trajectory density.

1) *Form of the Single-Trajectory Density*: The predicted and updated single-trajectory densities in the T-IEMB filter are of the form

$$p_{k|k'}^i(X) = \sum_{l=t^i}^k \beta_{k|k'}^i(l) p_{k|k'}^{i,l}(X) \quad (21)$$

where $\beta_{k|k'}^i(l)$ corresponds to the probability that the trajectory ends at time step l , and $p_{k|k'}^{i,l}(X)$ is a single-trajectory density ending at time step l . For the set of alive trajectories, $\beta_{k|k'}^i(k) = 1$ and $\beta_{k|k'}^i(l) = 0$ for $l \in \{t^i, \dots, k-1\}$, as we only consider trajectories that are alive at time step k . For the set of all trajectories, we consider trajectories that may

end at any time step $l \in \{t^i, \dots, k\}$, meaning each $p_{k|k'}^{i,l}(X)$ is weighted by its corresponding $\beta_{k|k'}^i(l)$. This results in a weighted mixture density where $\sum_{l=t^i}^k \beta_{k|k'}^i(l) = 1$.

2) *Update*: Given a predicted TMB density of the form (16), the posterior density can be found by applying a Bayesian update consisting of the prior and likelihood densities, which we write as

$$f_{k|k}(\mathbf{X}_k) = \frac{p(z_k|\mathbf{x}_k)f_{k|k-1}(\mathbf{X}_k)}{\int [p(z_k|\mathbf{x}_k)f_{k|k-1}(\mathbf{X}_k)] \delta \mathbf{X}_k} \quad (22)$$

where the integral is the set integral for trajectories (see Appendix A) [27]. The density (22) is not TMB, therefore the T-IEMB update stage computes a TMB approximation to the true non-TMB density (22).

To obtain the T-IEMB update, we follow the IEMB filter update [5]. Firstly, we introduce an auxiliary variable u to the single-trajectory space, such that the single-trajectory state is (u, X) . We define that each u takes a value in the space $\mathbb{U}_k = \{1, \dots, n_{k|k-1}\}$, and the single-trajectory state space then becomes $\mathbb{U}_k \times T_{(k)}$. A set of trajectories with auxiliary variables is denoted by $\tilde{\mathbf{X}}_k$. We then define

$$\tilde{\mathbf{X}}_k^i = \{(u, X) \in \tilde{\mathbf{X}}_k : u = i\}. \quad (23)$$

The predicted TMB density with auxiliary variables is then

$$\tilde{f}_{k|k-1}(\tilde{\mathbf{X}}_k) = \prod_{i=1}^{n_{k|k-1}} \tilde{f}_{k|k-1}^i(\tilde{\mathbf{X}}_k^i) \quad (24)$$

where each Bernoulli component with auxiliary variables is [29]

$$\tilde{f}_{k|k-1}^i(\tilde{\mathbf{X}}_k) = \begin{cases} 1 - r_{k|k-1}^i & \tilde{\mathbf{X}}_k = \emptyset \\ r_{k|k-1}^i p_{k|k-1}^i(X) \delta_i[u] & \tilde{\mathbf{X}}_k = \{(u, X)\} \\ 0 & \text{otherwise} \end{cases} \quad (25)$$

and the predicted TMB density of the form (16) reduces to (24) since the auxiliary variables ensure there is only one disjoint union of subsets of $\tilde{\mathbf{X}}_k$. We then aim to obtain an approximate TMB posterior of the form

$$\tilde{f}_{k|k}(\tilde{\mathbf{X}}_k) = \prod_{i=1}^{n_{k|k}} \tilde{f}_{k|k}^i(\tilde{\mathbf{X}}_k^i) \quad (26)$$

where each Bernoulli component $\tilde{f}_{k|k}^i(\tilde{\mathbf{X}}_k^i)$ is of the form (25).

Similarly to the proof for sets of targets [5, Appendix A], the MB approximation (26) which minimises the KLD between it and (22) (after adding the auxiliary variables), has Bernoulli components given by

$$\tilde{f}_{k|k}^u(\tilde{\mathbf{X}}_k^u) = \frac{p^u(z_k|\tilde{\mathbf{x}}_k^u)\tilde{f}_{k|k-1}(\tilde{\mathbf{X}}_k^u)}{\int p^u(z_k|\tilde{\mathbf{x}}_k^u)\tilde{f}_{k|k-1}(\tilde{\mathbf{X}}_k^u)\delta\tilde{\mathbf{X}}_k^u} \quad (27)$$

where $p^u(z_k|\tilde{\mathbf{x}}_k^u)$ is a modified likelihood for the u -th target, given by

$$\begin{aligned} p^u(z_k|\tilde{\mathbf{x}}_k^u) &= \int l(z_k|\mathbf{E}[z_k|\tilde{\mathbf{x}}_k], \mathbf{C}[z_k|\tilde{\mathbf{x}}_k]) \\ &\times \prod_{i=1:i \neq u}^{n_{k|k-1}} \tilde{f}_{k|k-1}^i(\tilde{\mathbf{x}}_k^i) \delta\tilde{\mathbf{x}}_k^{(-u)} \end{aligned} \quad (28)$$

where $\tilde{\mathbf{x}}_k = \tilde{\mathbf{x}}_k^1 \cup \dots \cup \tilde{\mathbf{x}}_k^{n_{k|k-1}}$ is the union of all targets, $\tilde{\mathbf{x}}_k^{(-u)} = (\tilde{\mathbf{x}}_k^1, \dots, \tilde{\mathbf{x}}_k^{u-1}, \tilde{\mathbf{x}}_k^{u+1}, \dots, \tilde{\mathbf{x}}_k^{n_{k|k-1}})$ is the sequence of sets of all targets excluding the u -th target, and the conditional moments $\mathbf{E}[z_k|\tilde{\mathbf{x}}_k]$ and $\mathbf{C}[z_k|\tilde{\mathbf{x}}_k]$ are the same as those without auxiliary variables. (28) integrates out the information from all Bernoulli components except the u -th one.

Each predicted single-target Bernoulli $\tilde{f}_{k|k-1}^i(\tilde{\mathbf{x}}_k^i)$ in (28) can be found from the corresponding trajectory Bernoulli $\tilde{f}_{k|k-1}^i(\tilde{\mathbf{X}}_k^i)$ with single-trajectory density (21) using the marginalisation theorem for TMB densities [38, Theorem 4], which gives

$$\tilde{f}_{k|k-1}^i(\tilde{\mathbf{x}}_k^i) = \begin{cases} r_{k|k-1}^i(k) p_{k|k-1}^i(x) & \tilde{\mathbf{x}}_k^i = \{(i, x)\} \\ 1 - r_{k|k-1}^i(k) & \tilde{\mathbf{x}}_k^i = \emptyset \\ 0 & \text{otherwise} \end{cases} \quad (29)$$

where the probability of existence of the target at time step k is

$$r_{k|k-1}^i(k) = r_{k|k-1}^i \beta_{k|k-1}^i(k) \quad (30)$$

and the single-target density is

$$p_{k|k-1}^i(x) = \int p_{k|k-1}^{i,k}(t^i, y^{1:k-t^i}, x) dy^{1:k-t^i} \quad (31)$$

which integrates out all previous target states in the single-trajectory density component that ends at time step k .

We now present the update for alive trajectories.

Lemma 3 (T-IEMB Update for Alive Trajectories). *Given a predicted TMB density of the form (24), the updated density is TMB of the form (26), where the updated single-trajectory density and probability of existence of the u -th Bernoulli is given by*

$$p_{k|k}^u(X) = \frac{p^u(z_k|\tau^k(X))p_{k|k-1}^{u,k}(X)}{\int p^u(z_k|\tau^k(X))p_{k|k-1}^{u,k}(X) dX} \quad (32)$$

$$r_{k|k}^u = \frac{p^u(z_k||\tilde{\mathbf{x}}_k^u| = 1)r_{k|k-1}^u}{p^u(z_k||\tilde{\mathbf{x}}_k^u| = 1)r_{k|k-1}^u + p^u(z_k|\emptyset)(1 - r_{k|k-1}^u)} \quad (33)$$

where $|\cdot|$ denotes the cardinality of a set, and $p^u(z_k||\tilde{\mathbf{x}}_k^u| = 1)$ is the likelihood of target existence

$$p^u(z_k||\tilde{\mathbf{x}}_k^u| = 1) = \int p^u(z_k|\{x_k\})p_{k|k-1}^u(x_k) dx_k \quad (34)$$

and $p^u(z_k|\emptyset)$ is given by (28) with $\tilde{\mathbf{x}}_k^u = \emptyset$.

We now present the update for all trajectories.

Lemma 4 (T-IEMB Update for All Trajectories). *Given a predicted TMB density of the form (24), the updated density is TMB of the form (26), where the updated single-trajectory density, updated probability of existence, and updated probability of the trajectory ending at time step $l \in \{t^u, \dots, k\}$ for the u -th Bernoulli is given by*

$$p_{k|k}^{u,l}(X) = \begin{cases} p_{k|k-1}^{u,l}(X) & l \in \{t^u, \dots, k-1\} \\ \frac{p^u(z_k|\tau^k(X))p_{k|k-1}^{u,l}(X)}{\int p^u(z_k|\tau^k(X))p_{k|k-1}^{u,l}(X) dX} & l = k \end{cases} \quad (35)$$

$$r_{k|k}^u = \frac{\rho_k^u r_{k|k-1}^u}{\rho_k^u r_{k|k-1}^u + (1 - r_{k|k-1}^u)p^u(z_k|\emptyset)} \quad (36)$$

$$\beta_{k|k}^u \propto \begin{cases} p^u(z_k|\emptyset)\beta_{k|k-1}^u(l) & l \in \{t^u, \dots, k-1\} \\ p^u(z_k||\tilde{\mathbf{x}}_k^u) = 1)\beta_{k|k-1}^u(l) & l = k \end{cases} \quad (37)$$

where

$$\rho_k^u = p^u(z_k||\tilde{\mathbf{x}}_k^u) = 1)\beta_{k|k-1}^u(k) + p^u(z_k|\emptyset) \sum_{l=t^u}^{k-1} \beta_{k|k-1}^u(l) \quad (38)$$

and $p^u(z_k||\tilde{\mathbf{x}}_k^u) = 1)$ is given by (34) and $p^u(z_k|\emptyset)$ by (28) with $\tilde{\mathbf{x}}_k^u = \emptyset$.

Lemma 4 is proved in Appendix B. It should be noted that if $\beta_{k|k-1}^u(k) = 1$, which corresponds to the case of alive trajectories and implies that $\beta_{k|k}^u(l) = 0$ for $l \in \{t^u, \dots, k-1\}$, then Lemma 4 reduces to Lemma 3, which is also proved.

IV. GAUSSIAN T-IEMB FILTER

We proceed to present the Gaussian implementation of the T-IEMB, termed GT-IEMB, for estimating the set of alive and all trajectories with the generalised superpositional measurement model of Section II-B. In this section we focus on the update as this is where our contributions lie. The prediction stage corresponds to the Gaussian implementation of the TMB filter [28] [29], which we include for alive and all trajectories in Appendix C for completeness.

We firstly detail the Gaussian trajectory densities in Section IV-A, along with the conditional moments of the generalised superpositional measurement model in Section IV-B. The conditional moments are used to develop the single-target Gaussian update in Section IV-C, which returns the updated single-target moments, where Section IV-D explains how single-trajectories can be updated using these. Finally, Sections IV-E and IV-F discuss practical considerations and trajectory estimation, respectively.

A. Gaussian Trajectory Densities

A Gaussian trajectory density with start time τ and duration ι is denoted by [29]

$$\mathcal{N}(t^i, x^{1:v}; \tau, \bar{x}, P) = \begin{cases} \mathcal{N}(x^{1:v}; \bar{x}, P) & t = \tau, v = \iota \\ 0 & \text{otherwise} \end{cases} \quad (39)$$

where the duration $\iota = \dim(\bar{x})/n_x$, where $\dim(\cdot)$ denotes dimensionality, the Gaussian trajectory density is evaluated at $(t^i, x^{1:v})$, with mean $\bar{x} \in \mathbb{R}^{\iota n_x}$ and covariance $P \in \mathbb{R}^{\iota n_x \times \iota n_x}$, and $\mathcal{N}(x; \mu, R)$ is a Gaussian density evaluated at x , with mean μ and covariance matrix R .

1) *Gaussian Single-Trajectory Density*: The Gaussian single-trajectory density (21) of the i th Bernoulli component in (16) is of the form

$$p_{k|k'}^i(X) = \sum_{l=t^i}^k \beta_{k|k'}^i(l) \mathcal{N}(X; t^i, \bar{x}_{k|k'}^i(l), P_{k|k'}^i(l)) \quad (40)$$

where t^i is the trajectory start time, $\bar{x}_{k|k'}^i(l) \in \mathbb{R}^{\iota n_x}$ is the trajectory mean ending at time step l , and $P_{k|k'}^i(l) \in \mathbb{R}^{\iota n_x \times \iota n_x}$

$\mathbb{R}^{\iota n_x}$ is the covariance matrix for the trajectory ending at time step l , where $\iota = l - t^i + 1$. For the set of alive trajectories, $\beta_{k|k'}^i(k) = 1$ and $\beta_{k|k'}^i(l) = 0$ for $l \in \{t^i, \dots, k-1\}$. For the set of all trajectories, we have a weighted Gaussian mixture density where $\sum_{l=t^i}^k \beta_{k|k'}^i(l) = 1$.

2) *Gaussian Single-Target Density*: The T-IEMB filter updates for alive and all trajectories (Lemmas 3 and 4) require updating the single-trajectory density component that is alive, denoted by $p_{k|k-1}^{i,k}(X)$, while the rest of the single-trajectory density components remain unchanged. In the Gaussian implementation, $p_{k|k-1}^{i,k}(X)$ has trajectory mean $\bar{x}_{k|k-1}^i(k)$ and covariance matrix $P_{k|k-1}^i(k)$.

As the likelihood depends only on the current single-target states, we perform the update by first updating the single-target density $p_{k|k-1}^{i,k}(x)$ at time step k associated with the single-trajectory density $p_{k|k-1}^{i,k}(X)$. This density is Gaussian with a density

$$p_{k|k-1}^{i,k}(x) = \mathcal{N}(x; \mu_{k|k-1}^i, \Xi_{k|k-1}^i) \quad (41)$$

where its mean $\mu_{k|k-1}^i \in \mathbb{R}^{\iota n_x}$ and covariance matrix $\Xi_{k|k-1}^i \in \mathbb{R}^{\iota n_x \times \iota n_x}$ are directly obtained from the trajectory mean and covariance matrix. We explain how to compute the updated mean $\mu_{k|k}^i$ and covariance $\Xi_{k|k}^i$ in Section IV-C, for which we first require the conditional moments of the measurement in Section IV-B. Finally, we explain how to update past states of the trajectories in Section IV-D.

B. Conditional Moments of the Measurement

The Gaussian update for the u -th target, following [31], requires the conditional measurement mean and covariance given the target set $\tilde{\mathbf{x}}^u$. We firstly introduce the following variables and their moments that will be required for the update. Given a single-target $\tilde{\mathbf{x}}^i$, we define these internal variables related to the measurement model (7)

$$h^i = \begin{cases} h(x) & \tilde{\mathbf{x}}^i = \{(i, x)\} \\ 0 & \tilde{\mathbf{x}}^i = \emptyset \end{cases} \quad (42)$$

$$R^i = \begin{cases} R(x) & \tilde{\mathbf{x}}^i = \{(i, x)\} \\ 0 & \tilde{\mathbf{x}}^i = \emptyset \end{cases} \quad (43)$$

Lemma 5. Given an MB predicted density of the form (16) with single-trajectory densities of the form (40), the mean and covariance of h^i , and the mean of R^i , are

$$\mathbb{E}[h^i] = r_{k|k-1}^i(k) \mathbb{E}_i[h(x)] \quad (44)$$

$$\begin{aligned} \mathbb{C}[h^i] &= r_{k|k-1}^i(k) \mathbb{E}_i[h(x)h(x)^T] \\ &\quad - (r_{k|k-1}^i(k))^2 \mathbb{E}_i[h(x)] (\mathbb{E}[h(x)])^T \end{aligned} \quad (45)$$

$$\mathbb{E}[R^i] = r_{k|k-1}^i(k) \mathbb{E}_i[R(x)] \quad (46)$$

where $r_{k|k-1}^i(k)$ is given by (30), and

$$\mathbb{E}_i[h(x)] = \int h(x) p_{k|k-1}^{i,k}(x) dx \quad (47)$$

$$\mathbb{E}_i[R(x)] = \int R(x) p_{k|k-1}^{i,k}(x) dx \quad (48)$$

$$\mathbb{E}_i[h(x)h(x)^T] = \int h(x)(h(x))^T p_{k|k-1}^{i,k}(x) dx. \quad (49)$$

A proof of the results in Lemma 5 is provided in Appendix D. We next define the additive internal variables across all targets except the u -th target, which we denote

$$h^{(-u)} = \sum_{i=1:i \neq u}^{n_{k|k-1}} h^i \quad (50)$$

$$R^{(-u)} = \sum_{i=1:i \neq u}^{n_{k|k-1}} R^i. \quad (51)$$

Since the variables inside the sums in (50) and (51) are independent, we directly obtain the following lemma.

Lemma 6. *Given an MB predicted density of the form (16) with single-trajectory densities of the form (40), the mean and covariance of $h^{(-u)}$, and the mean of $R^{(-u)}$, are*

$$\hat{h}_{corr}^u = E[h^{(-u)}] = \sum_{i=1:i \neq u}^{n_{k|k-1}} E[h^i] \quad (52)$$

$$S_{corr}^u = C[h^{(-u)}] = \sum_{i=1:i \neq u}^{n_{k|k-1}} C[h^i] \quad (53)$$

$$R_{corr}^u = E[R^{(-u)}] = \sum_{i=1:i \neq u}^{n_{k|k-1}} E[R^i] \quad (54)$$

where $E[h^i]$, $C[h^i]$ and $E[R^i]$ are given by (44), (45) and (46), respectively.

To perform the update of the u th Bernoulli, we require the conditional moments $E[z_k|\tilde{\mathbf{x}}_k^u = \{(u, x^u)\}]$ and $C[z_k|\tilde{\mathbf{x}}_k^u = \{(u, x^u)\}]$ [31]. For computational efficiency, we derive approximations of these moments via Taylor series expansion of $m(\cdot)$ and $R(\cdot)$. We do these expansions such that in the filter implementation we can approximate the required integrals for each potential target by only drawing sigma-points from the distribution of this potential target, improving the computational efficiency of the algorithm.

Given the result of Lemma 6, the first-order Taylor series expansion of $m(h(x^u) + h^{(-u)})$ around the point $h(x^u) + \hat{h}_{corr}^u$ is given by

$$m(h(x^u) + h^{(-u)}) \approx m(h(x^u) + \hat{h}_{corr}^u) + M(h(x^u) + \hat{h}_{corr}^u)(h^{(-u)} - \hat{h}_{corr}^u) \quad (55)$$

where $M(h(x^u) + \hat{h}_{corr}^u)$ is the Jacobian of $m(\cdot)$ evaluated at $h(x^u) + \hat{h}_{corr}^u$. In addition, the zero-order Taylor series expansion of $\Sigma(R(x^u) + R^{(-u)})$ around $R(x^u) + R_{corr}^u$ is given by

$$\Sigma(R(x^u) + R^{(-u)}) \approx \Sigma(R(x^u) + R_{corr}^u). \quad (56)$$

Proposition 7. *Under approximation (55), the conditional mean of z_k given $\tilde{\mathbf{x}}_k^u = \{(u, x^u)\}$ is*

$$E[z_k|\tilde{\mathbf{x}}_k^u = \{(u, x^u)\}] \approx m(h(x^u) + \hat{h}_{corr}^u). \quad (57)$$

Under approximations (55) and (56), the conditional covariance of z_k given $\tilde{\mathbf{x}}_k^u = \{(u, x^u)\}$ is

$$C[z_k|\tilde{\mathbf{x}}_k^u = \{(u, x^u)\}] \approx \Sigma(R(x^u) + R_{corr}^u)$$

$$+ M(h(x^u) + \hat{h}_{corr}^u)S_{corr}^uM(h(x^u) + \hat{h}_{corr}^u)^T. \quad (58)$$

For the case $\tilde{\mathbf{x}}_k^u = \emptyset$, the conditional moments are approximated as

$$E[z_k|\tilde{\mathbf{x}}_k^u = \emptyset] \approx m(\hat{h}_{corr}^u) \quad (59)$$

$$C[z_k|\tilde{\mathbf{x}}_k^u = \emptyset] \approx \Sigma(R_{corr}^u) + M(\hat{h}_{corr}^u)S_{corr}^uM(\hat{h}_{corr}^u)^T. \quad (60)$$

A proof is provided in Appendix E.

C. Single-Target Gaussian Update

1) *Enabling Approximation:* To perform a Gaussian update of the measurement model with conditional moments (57) and (58), we must first approximate the non-linear and non-Gaussian measurement into a linear and Gaussian form [39]. We can view the measurement (conditioned on a single-target $\tilde{\mathbf{x}}_k^u = \{(u, x^u)\}$) as a transformation of the state x^u by a non-linear function $g(\cdot)$, with a state dependent zero-mean noise term $\eta(\cdot)$ additive to this transformation, which can be written as [40]

$$z_k = g(x^u) + \eta(x^u) \quad (61)$$

where $g(x^u) = E[z_k|\tilde{\mathbf{x}}_k^u = \{(u, x^u)\}]$, given by (57), and $\eta(x^u)$ has covariance matrix $\Psi(x^u) = C[z_k|\tilde{\mathbf{x}}_k^u = \{(u, x^u)\}]$, given by (58).

Considering the measurement as (61), we form a linear and Gaussian approximation using the following enabling approximation

$$z_k \approx Ax^u + b + r \quad (62)$$

where $A \in \mathbb{R}^{Mn_z \times n_x}$, $b \in \mathbb{R}^{Mn_z}$ are linearisation parameters, and $r \in \mathbb{R}^{Mn_z}$ is a zero-mean Gaussian noise term with covariance matrix $\Omega \in \mathbb{R}^{n_z \times n_z}$. We clarify that (A, b) provide an affine transformation which forms a linear approximation to the conditional mean (57), and the Gaussian noise term r has covariance matrix Ω which accounts for both the linearisation error, and the conditional covariance of the measurement (58). Given (62), the Kalman filter (KF) provides us with the updated mean $\mu_{k|k}^u$ and covariance $\Xi_{k|k}^u$ [41]

$$K^u = \Xi_{k|k-1}^u A^T (A \Xi_{k|k-1}^u A^T + \Omega)^{-1} \quad (63)$$

$$\mu_{k|k}^u = \mu_{k|k-1}^u + K^u(z_k - A\mu_{k|k-1}^u + b) \quad (64)$$

$$\Xi_{k|k}^u = \Xi_{k|k-1}^u - K^u(A \Xi_{k|k-1}^u A^T + \Omega)(K^u)^T. \quad (65)$$

Finally, the target probability of existence can be computed using (33), which requires the likelihoods of existence and non-existence. Under the Gaussian approximation of the measurement (61) (with moments defined in (57) and (58)), the likelihood of existence is

$$p^u(z_k || \tilde{\mathbf{x}}_k^u = 1) = \mathcal{N}(z_k; A\mu_{k|k-1}^u + b, A\Xi_{k|k-1}^u A^T + \Omega). \quad (66)$$

Under a Gaussian approximation of the measurement when the u -th target is not present, using (59) and (60), the likelihood of non-existence is

$$p^u(z_k | \emptyset) = \mathcal{N}(z_k; m(\hat{h}_{corr}^u), \Sigma(R_{corr}^u) + M(\hat{h}_{corr}^u)S_{corr}^uM(\hat{h}_{corr}^u)^T). \quad (67)$$

The parameters (A, b, Ω) are determined using Statistical Linear Regression (SLR), which is explained in the next section.

2) *SLR using Sigma Points*: To perform a closed form Gaussian update, we require the linear and Gaussian approximation to the measurement (62). The required parameters (A, b, Ω) are found using SLR, which returns an optimal linearisation of the nonlinear function $g(\cdot)$ with respect to some density $\mathcal{N}(x; \bar{x}, P)$. More specifically, SLR minimises the mean squared error between the linear and Gaussian approximation of the function, and its exact nonlinear and non-Gaussian form. This minimisation is posed as an optimisation problem, in which the optimal linearisation parameters which minimise the mean squared error are returned. We can write this as

$$\begin{aligned} (A^+, b^+) &= \arg \min_{(A, b)} \mathbb{E} [\|g(x^u) + \eta(x^u) - A^+ x^u - b^+\|^2] \\ &= \arg \min_{(A, b)} \mathbb{E} [\|g(x^u) - A^+ x^u - b^+\|^2] \end{aligned} \quad (68)$$

where the zero-mean noise $\eta(x^u)$ can be removed as this is uncorrelated with $g(x^u)$ [31]. Solving this optimisation problem gives [39]

$$A^+ = \mathbb{C}[x, g(x)]^T P^{-1} \quad (69)$$

$$b^+ = \mathbb{E}[g(x)] - A^+ \bar{x}^u. \quad (70)$$

The zero-mean Gaussian noise term $\eta(x^u)$ has covariance matrix Ω equal to the mean square error matrix, which is found to be [40]

$$\begin{aligned} \Omega &= \mathbb{E}[(g(x) - Ax^u - b)(g(x) - Ax^u - b)^T] \\ &\quad + \mathbb{E}[\eta(x^u)\eta(x^u)^T] \\ &= \mathbb{C}[g(x^u)] + \mathbb{E}[\Psi(x^u)] - A^+ P (A^+)^T. \end{aligned} \quad (71)$$

The moments required to evaluate (69)-(71) are intractable in practice, therefore must be approximated using a suitable method.

3) *Application of SLR to IEMB Update Step* : The parameters (A, b, Ω) approximate the conditional moments of the measurement (57) and (58), which contain the correction moments \hat{h}_{corr}^u , R_{corr} and S_{corr}^u that account for the influence of all other targets on the measurement. Given this, we must firstly estimate the correction moments before proceeding with SLR.

We adopt a sigma-point based approach for estimating both the correction moments, and the moments required to perform SLR using (69)-(71). Alternative approaches could be employed, such as a Taylor series expansion (as is used for performing SLR in [40] and [42]), however we only detail an Unscented Transform based [41] approach here.

To estimate the correction moments, we draw a set of $m_s = 2n_x + 1$ sigma-points denoted $\mathcal{X}^1, \dots, \mathcal{X}^{m_s}$ with corresponding weights $\omega^1, \dots, \omega^{m_s}$, with respect to each i th predicted single-target density $\mathcal{N}(x^i; \mu_{k|k-1}^i, \Xi_{k|k-1}^i)$. The sigma-points and weights are drawn using an appropriate method [41, Chapter 5], which are then used to approximate the following moments

$$\mathbb{E}_i[h(x)] \approx \sum_{s=1}^{m_s} \omega^s h(\mathcal{X}^s) \quad (72)$$

Algorithm 1 SLR of Generalised Superpositional Measurement Model for the u -th Target.

Input : \bar{x} , P , \hat{h}_{corr}^u , R_{corr}^u and S_{corr}^u

Output : (A, b, Ω)

- Draw m_s sigma points $\mathcal{X}^1, \dots, \mathcal{X}^{m_s}$ and corresponding weights which match \bar{x} , P using an appropriate method e.g. [41, Chapter 8].
- Transform the set of sigma points through the nonlinear functions in (57) and (58) to

$$\mathcal{G}^s = m(h(\mathcal{X}^s) + \hat{h}_{corr}^u)$$

$$\mathcal{R}^s = \Sigma(R(\mathcal{X}^s) + R_{corr}^u)$$

$$\mathcal{M}^s = M(h(\mathcal{X}^s) + \hat{h}_{corr}^u).$$

- Approximate the following moments

$$\mathbb{E}[g(x)] \approx \sum_{s=1}^{m_s} \omega^s \mathcal{G}^s, \quad \mathbb{E}[g(x)g(x)^T] \approx \sum_{s=1}^{m_s} \omega^s \mathcal{G}^s (\mathcal{G}^s)^T$$

$$\mathbb{C}[g(x)] = \mathbb{E}[g(x)g(x)^T] - \mathbb{E}[g(x)]\mathbb{E}[g(x)]^T$$

$$\mathbb{C}[x, g(x)] \approx \sum_{s=1}^{m_s} \omega^s (\mathcal{X}^s - \bar{x})(\mathcal{G}^s - \mathbb{E}[g(x)])^T$$

$$\mathbb{E}[\Psi(x)] = \mathbb{E}[\Sigma(R(x) + R_{corr}^u)] +$$

$$\mathbb{E}[M(h(x) + \hat{h}_{corr}^u) S_{corr}^u M(h(x) + \hat{h}_{corr}^u)^T]$$

$$\mathbb{E}[\Sigma(R(x) + R_{corr}^u)] \approx \sum_{s=1}^{m_s} \omega^s \mathcal{R}^s$$

$$\mathbb{E}[M(h(x) + \hat{h}_{corr}^u) S_{corr}^u M(h(x) + \hat{h}_{corr}^u)^T] \approx \sum_{s=1}^{m_s} \omega^s \mathcal{M}^s S_{corr}^u (\mathcal{M}^s)^T.$$

- Compute (A, b, Ω) using $\mathbb{E}[g(x)]$, $\mathbb{C}[g(x)]$, $\mathbb{C}[x, g(x)]$ and $\mathbb{E}[\Psi(x)]$ in (69)-(71).

$$\mathbb{E}_i[h(x)h(x)^T] \approx \sum_{s=1}^{m_s} \omega^s h(\mathcal{X}^s) (h(\mathcal{X}^s))^T \quad (73)$$

$$\mathbb{E}_i[R(x)] \approx \sum_{s=1}^{m_s} \omega^s R(\mathcal{X}^s) \quad (74)$$

which are required in the correction moments (52)-(54). Calculation of (72)-(74) is repeated for $i = 1 : n_{k|k-1}$, such that we can calculate the correction moments for each u -th target. We can then proceed to execute Algorithm 1 with \hat{h}_{corr}^u , R_{corr}^u and S_{corr}^u , which performs SLR of the measurement (61) conditioned on the u -th target, and returns the parameters (A, b, Ω) with respect to some density with mean \bar{x} and covariance P .

4) *IPLF*: Executing Algorithm 1 with respect to $\mathcal{N}(x^u; \mu_{k|k-1}^u, \Xi_{k|k-1}^u)$ returns (A, b, Ω) with respect to the prior, and performing the update (63)-(65) using this parameter set is then equivalent to an Unscented KF (UKF) update. An improved update can be performed using the IPLF [34], which performs iterated SLR with respect to the best estimate of the target posterior density at each iteration.

The first iteration of SLR using Algorithm 1 is performed with respect to $\mathcal{N}(x^u; \mu_{k|k-1}^u, \Xi_{k|k-1}^u)$, which re-

Algorithm 2 T-IEMB-IPLF Update for Each u -th Target

Input: Predicted Bernoulli components for $u = 1 : n_{k|k-1}$.

Output: Updated Bernoulli components for $u = 1 : n_{k|k}$.

For $i = 1 : n_{k|k-1}$

- Draw sigma points $\mathcal{X}^{1:m_s}$ and weights $\omega^{1:m_s}$ matching $\mu_{k|k-1}^i$ and $\Xi_{k|k-1}^i$.
- Calculate $E_i[h(x)]$, $E_i[h(x)h(x)]$ and $E_i[R(x)]$ in (72)–(74) using $\mathcal{X}^{1:m_s}$ and $\omega^{1:m_s}$.

End

For $u = 1 : n_{k|k-1}$

- Calculate \hat{z}_{corr}^u , R_{corr}^u and S_{corr}^u using (52)–(54).

End

For $u = 1 : n_{k|k-1}$

- Set $\bar{x} = \mu_{k|k-1}^u$ and $P = \Xi_{k|k-1}^u$.

Repeat:

- Execute Algorithm 1 with inputs \bar{x} , P and \hat{z}_{corr}^u , R_{corr}^u , S_{corr}^u to compute (A^i, b^i, Ω^i) .
- Calculate the updated mean $\mu_{k|k}^{u,i}$ and covariance $\Xi_{k|k}^{u,i}$ using (A^i, b^i, Ω^i) in (63)–(65).
- Set $\bar{x} = \mu_{k|k}^{u,i}$ and $P = \Xi_{k|k}^{u,i}$.

Until: Fixed number of iterations or KLD convergence [34, Section IV-D].

- Compute $p^u(z_k || \bar{x}_k^u) = 1$ and $p^u(z_k || \emptyset)$ using (66) and (67), respectively. Then for alive trajectories, update $r_{k|k}^u$ using (33), and for all trajectories update $r_{k|k}^u$ using (36) and $\beta_{k|k}^u(l)$ using (37).
- Update mean and covariance of past trajectory states, see Appendix F.

End

turns (A^1, b^1, Ω^1) with respect to the prior target density. The updated moments are computed using (63)–(65) using (A^1, b^1, Ω^1) , which returns the posterior target density $\mathcal{N}(x^u; \mu_{k|k}^{u,1}, \Xi_{k|k}^{u,1})$. Algorithm 1 is then executed again with respect to $\mathcal{N}(x^u; \mu_{k|k}^{u,1}, \Xi_{k|k}^{u,1})$, which returns a new set of SLR parameters, which are then used to compute the next target posterior estimate. This process is repeated for some number of iterations, which then returns a posterior target density computed using (A, b, Ω) with respect to the latest estimate of the target posterior. A complete derivation and convergence analysis of the IPLF is provided in [34]. Algorithm 2 details the complete T-IEMB-IPLF update stage for each single-target using the generalised superpositional measurement model.

D. GT-IEMB Single-Trajectory Gaussian Update

1) *Alive Trajectories:* With a predicted TMB density of the form (16), we perform the update of the GT-IEMB using a state decomposition approach. That is, we compute the single-target updated density $p_{k|k}^{i,k}(x)$ corresponding to the target state at time step k of trajectory density $p_{k|k}^{i,k}(X)$ using the update outlined in Section IV-C. This returns the updated single-target moments $\mu_{k|k}^i$ and $\Xi_{k|k}^i$, which can then be used to update past trajectory states using the approach detailed in Appendix F, see also [43] [44]. Finally, the updated existence probability

$r_{k|k}^i$ is computed with (33), using the existence likelihoods (66) and (67).

2) *All Trajectories:* Given a predicted TMB density of the form (16), we obtain the updated single-target moments $\mu_{k|k}^i$ and $\Xi_{k|k}^i$ following the same approach as for the update of alive trajectories, presented in Section IV-D1. These moments are then used to update the past states of the trajectory following Appendix F. We note that, the updated trajectory density $p_{k|k-1}^{i,l}(X)$ for $l \in \{t^i, \dots, k-1\}$ is given by its predicted trajectory density i.e. we do not perform any update, as these represent trajectories which ended at a previous time step. The updated existence probability $r_{k|k}^i$ is then found using (36), and the updated Beta parameters $\beta_{k|k}^i(l)$ for $l \in \{t^i, \dots, k\}$ are found using (37).

E. Practical Considerations

As the trajectory length increases, the update becomes increasingly computationally expensive. As a practical approximation, which is employed in the other trajectory based filters e.g. [28]–[30], we use the L -scan approximation which limits the update of a trajectory to a window of L time steps. That is, when performing the past trajectory update using Appendix F, we update only the last L time steps, which limits computational cost of the trajectory update. We also bound the size of the covariance matrix to $L n_x \times L n_x$, which is consistent with an update of the last L time steps.

For the set of alive trajectories, we discard Bernoulli components whose updated existence probability $r_{k|k}^i$ is below some threshold Γ_d , which indicates there is very low probability of the trajectory being alive. For the set of all trajectories, we again discard Bernoulli components with updated existence probability below Γ_d , however Bernoulli components once considered alive will always have a high existence probability. Given this, $\beta_{k|k}^i(k)$ is used to indicate the probability that the trajectory is still alive i.e. if $\beta_{k|k}^i(k)$ is very low then there is very high probability the trajectory ended at a previous time step $l \in \{t^i, \dots, k-1\}$. Therefore, if $\beta_{k|k}^i(k)$ is less than some threshold Γ_a , we set $\beta_{k|k}^i(k) = 0$ which indicates that the trajectory has died, and it is no longer updated (but is still held in the set of all trajectories).

F. Estimation

Given the T-IEMB posterior (26) at any time step, we use the following estimators to extract the corresponding sets of alive and all trajectories (which follows the strategy of the estimators in [29]). For the set of alive trajectories at time step k , each alive trajectory is given from the T-IEMB posterior as $\{(t^i, \bar{x}_{k|k}^i) : r_{k|k}^i > \Gamma_d\}$, meaning the set of alive trajectories comprises of each trajectory with existence probability above the set threshold Γ_d .

For the set of all trajectories at time step k , the set comprises of each trajectory from the T-IEMB posterior given as $\{(t^i, \bar{x}_{k|k}^i(l^*)) : r_{k|k}^i > \Gamma_d, l^* = \arg \max_l \beta_{k|k}^i(l)\}$. This gives each trajectory ending at the time step with the highest value of $\beta_{k|k}^i(l)$, and also each trajectory has existence probability greater than the threshold Γ_d .

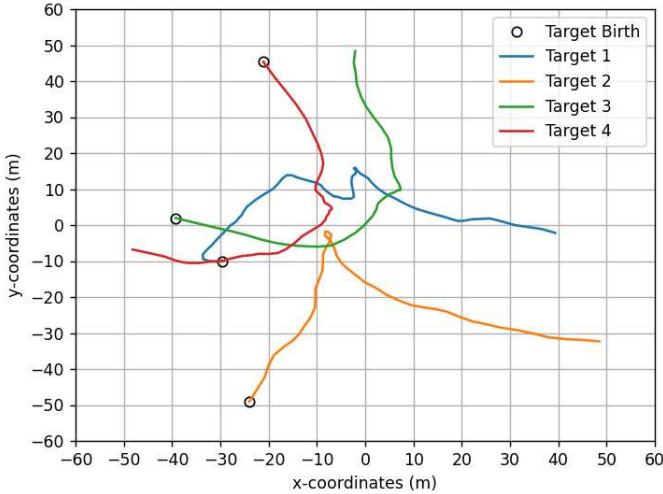


Figure 3: Ground truth trajectories of each target, where targets 1 through 4 are born at time steps 3, 16, 17, and 20, respectively, and die at time steps 74, 64, 57 and 64, respectively. Each radar resolution cell is of dimensions $10 \text{ m} \times 10 \text{ m}$, which is illustrated using the grid.

V. SIMULATIONS

We illustrate our filtering concept by considering a non-Gaussian TkBD scenario. We first detail the target dynamic model and non-Gaussian measurements in Sections V-A and V-B, respectively, before detailing the considered filters and performance metric in Section V-C. Simulation results and their discussion are then provided in Section V-D.

A. Target Dynamic Model

A surveillance area of dimension $120 \text{ m} \times 120 \text{ m}$ contains four targets, as illustrated in Figure 3. Each target is described by its state vector $x_k = [p_{x,k}, v_{x,k}, p_{y,k}, v_{y,k}]^T$, where $p_{x,k}$ and $v_{x,k}$ are the target position and velocity in the x-axis at time step k , respectively. Each target survives to the next time step with probability of survival $p^S = 0.99$, with state evolution between time steps modelled by a nearly constant velocity model, where [45]

$$F = I_2 \otimes \begin{bmatrix} 1 & T \\ 0 & 1 \end{bmatrix}, \quad Q = \sigma_q^2 I_2 \otimes \begin{bmatrix} \frac{T^3}{2} & \frac{T^2}{2} \\ \frac{3}{2} & T \end{bmatrix} \quad (75)$$

are the state transition function and process noise covariance, respectively. We note that I_2 denotes the two dimensional identity matrix, \otimes denotes the Kronecker product, $T = 1 \text{ s}$ is the sampling period, and $\sigma_q = 0.5 \text{ m}^2/\text{s}^3$ is the process noise variance. In the prediction step, $n^{b_k} = 1$ Bernoulli birth components are introduced (2), which have a mean, covariance and birth probability of $m_k^b = [0, 0, 0, 0]^T$, $P_k^b = \text{diag}([200, 10, 200, 10])$ and $p_k^b = 10^{-6}$, respectively. This birth model is uninformative, and covers a large area as there is no prior information on target birth locations.

B. Rician Distributed Measurements

For our simulations we use an alternative formulation of the generalised measurement model in Section II-B. We assume

that each sensor measurement z_k^j is independent given the target state with the factorisation

$$p(z_k | \mathbf{x}_k) = \prod_{j=1}^M p(z_k^j | \mathbf{x}_k). \quad (76)$$

This implies that (5) and (6) can be defined for each sensor j , with inputs $h^j(\cdot)$, $m^j(\cdot)$, $R^j(\cdot)$ and $\Sigma^j(\cdot)$ which consider each sensor separately. The conditional moments for each sensor can then be stacked (analogously to (3) and (4)) to form the conditional moments of the measurement vector.

We consider a radar surveillance scenario, in which a surveillance area is segmented into M individual cells, where the centre of cell $j \in \{1, \dots, M\}$ has coordinates (c_x^j, c_y^j) in the x and y dimensions, respectively. Each target in the surveillance area is assumed to possess a constant RCS i.e. Swerling 0 targets, and clutter is assumed to be Rayleigh distributed, which is a common radar assumption. At each time step k , a radar return signal z_k^j is measured from each cell, where the density of the measurement z_k^j given the set of targets \mathbf{x}_k is Rician of the form [32, Chapter 8]

$$p(z_k^j | \mathbf{x}_k) = \frac{z_k^j}{\sigma_r^2} \exp \left(-\frac{(z_k^j)^2 + (\lambda^j)^2}{2\sigma_r^2} \right) I_0 \left(\frac{z_k^j \lambda^j}{\sigma_r^2} \right) \quad (77)$$

where $\sigma_r = 2$, $\lambda^j = \sum_{x_k \in \mathbf{x}_k} h^j(x_k)$ where $h^j(x_k)$ is the return signal from target x_k in cell j , and $I_0(\cdot)$ is the modified Bessel function of the first kind of order 0. The Rice density (77) describes the measurement density of fixed RCS targets in the presence of Rayleigh clutter [32, Chapter 8]. Target returns from each cell are modelled using the Gaussian Point Spread Function (PSF)

$$h^j(x_k) = \varphi \exp \left(-\frac{(c_x^j - p_{x,k})^2}{2\sigma_x^2} - \frac{(c_y^j - p_{y,k})^2}{2\sigma_y^2} \right) \quad (78)$$

where $\varphi = 10$ is the maximum target return signal, and $\sigma_x = \sigma_y = 10$ is the variance of the PSF in each dimension (which defines the spatial extent of the target signature). We note that the normalisation constant of the PSF has been removed such that the maximum value is unity.

Under the alternative formulation of the measurement model, the conditional moments are defined for each cell j using the measurement function for each cell (78). Given the Rician distributed measurement (77), the conditional moments of each cell can be formulated using the known result of the Rice distribution mean and covariance [46], which gives

$$\mathbb{E}[z_k^j | \mathbf{x}_k] = m^j(\lambda^j) = \sigma_r \sqrt{\frac{\pi}{2}} L_{1/2} \left(-\frac{(\lambda^j)^2}{2\sigma_r^2} \right) \quad (79)$$

$$\mathbb{C}[z_k^j | \mathbf{x}_k] = \Sigma^j(\lambda^j) = 2\sigma_r^2 + (\lambda^j)^2 - (\mathbb{E}[z_k^j | \mathbf{x}_k])^2 \quad (80)$$

where $L_{1/2}(\cdot)$ denotes the Laguerre polynomial [47, Chapter 22]. We provide further information regarding the moments of the Rician distributed measurements in Appendix G.

C. Algorithms and Performance Assessment

For our simulations we consider two implementations of the GT-IEMB, the T-IEMB-UKF and T-IEMB-IPLF. We also

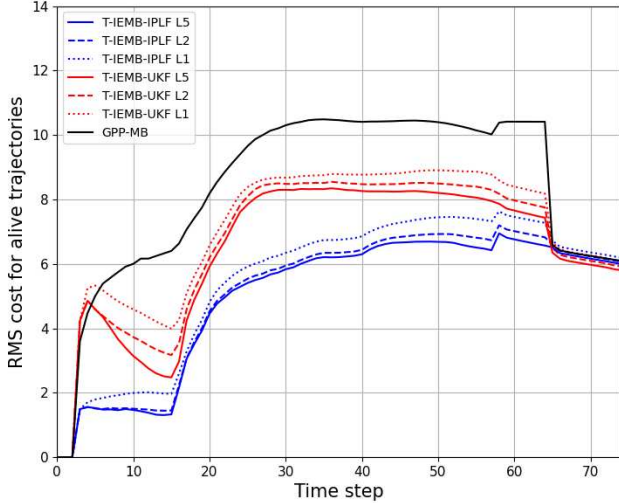


Figure 4: Total RMS T-GOSPA cost of each filter for the set of alive trajectories. Lx denotes a filter with an L -scan length of x .

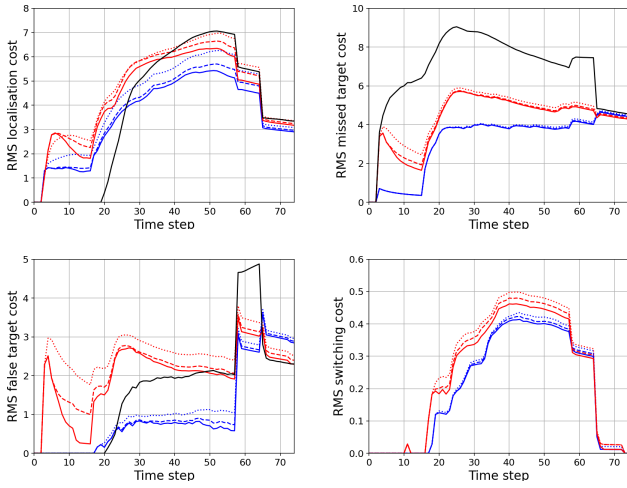


Figure 5: (clockwise from top left) RMS T-GOSPA localisation, missed, switch and false cost of each filter (legend is included in Figure 4).

consider the Trajectory Independent Multi-Bernoulli (T-IMB) filter [48], which does not exchange any information between filters, with both a UKF and IPLF implementation. We use only an L -scan length of 1 to serve as a performance baseline. Both the UKF and IPLF use sigma-points with a central weight $\omega_0 = \frac{1}{3}$, and the IPLF is set to a maximum of 20 iterations with a KLD threshold of 10^{-1} . For the set of alive trajectories, we prune trajectories with an updated existence probability $r_{k|k}$ below $\Gamma_d = 0.01$, and for the set of all trajectories we do not update trajectories whose updated termination probability $\beta_{k|k}(k)$ is below $\Gamma_a = 0.01$. Both GT-IEMB and T-IMB implementations were written using Python 3.12¹.

We also compare the TMB based filters against the Generalised Parallel Partition Multi-Bernoulli (GPP-MB) filter [14], a multi-target particle filter for TkBD, written using MATLAB and MEX. The GPP-MB was implemented using 1000 particles for each target, and uses a sequential track-building approach to build tracks from its sequential single-

target estimates. We cannot compare with the Gaussian implementations of the IEMB filter [5] and the IMB filter [48] since these implementations cannot handle the considered measurement model.

To assess filter performance we use the Trajectory Generalised Optimal Sub-pattern Assignment (T-GOSPA) metric [49], denoted $d(\cdot, \cdot)$. T-GOSPA cost is decomposed into four individual sources, namely localisation, missed, false and switch costs. The metric parameters used were $p = 2$, $c = W$ where W is the radar resolution cell width, and $\gamma = 1$. We use an online T-GOSPA implementation for producing graphical results, where we normalise the metric result at each time step k considering the set of trajectory estimates $\hat{\mathbf{X}}_k$ and true trajectories \mathbf{X}_k . The Root Mean Squared (RMS) value of the metric at each time step k over $N_{mc} = 100$ Monte Carlo (MC) runs is then given by

$$d(k) = \sqrt{\frac{1}{N_{mc}k} \sum_{i=1}^{N_{mc}} d^2(\mathbf{X}_k, \hat{\mathbf{X}}_k^i)}. \quad (81)$$

We also generate tabulated results, where the RMS average metric result over a scenario with T time steps is given by

$$d_T = \sqrt{\frac{1}{T} \sum_{k=1}^T d^2(k)}. \quad (82)$$

D. Simulation Results

Figure 4 shows the total RMS T-GOSPA cost for three considered filters when estimating the set of alive trajectories, with varying L -scan lengths for each GT-IEMB implementation. The T-IMB filter implementations perform worse than the rest and are omitted in the figures for clarity, with tabulated results provided instead. GPP-MB performance is worst, while the T-IEMB-UKF improves on the GPP-MB, and the T-IEMB-IPLF provides best performance of the three. Increasing the L -scan length for each trajectory-based filter also reduces their respective costs. Figure 5 shows the T-GOSPA cost decomposition for each filter considered in Figure 4, which allows for a more thorough analysis of each filters performance.

Localisation cost reduces when increasing the L -scan length for both the UKF and IPLF implementation, as the update of past states improves localisation over time. Localisation is reduced for the IPLF implementation as compared to the UKF, as its iterative update provides a higher accuracy estimate of the target posterior density. The primary performance difference between each GT-IEMB implementation is in missed and false target cost. The IPLFs iterative update means the highly nonlinear update of a birth component is performed over multiple iterations, whereas the UKF must complete this update in a single iteration. The IPLF implementation is therefore superior at initialising new trajectories, which is evident from the reduced missed target cost over the scenario. False target cost is also reduced for the IPLF implementation, owing to an increased accuracy estimate of the target posterior.

The increased cost for the GPP-MB is mainly influenced by a high missed target cost, since it uses an uninformative birth

¹T-IEMB Python code will be made available once the paper is accepted.

Table I: RMS T-GOSPA Cost for Alive Trajectories

L -scan	GPP-MB	T-IMB-UKF	T-IMB-IPLF	T-IEMB-UKF					T-IEMB-IPLF				
				1	2	5	10	15	1	2	5	10	15
Total	8.70	21.64	24.98	7.39	7.04	6.86	6.80	6.80	5.91	5.56	5.40	5.42	5.42
Localisation	4.61	5.07	5.27	5.05	4.89	4.69	4.66	4.65	4.43	4.03	3.83	3.86	3.86
Missed	7.06	5.69	6.01	4.70	4.51	4.48	4.45	4.45	3.56	3.52	3.50	3.50	3.50
False	2.13	20.24	23.65	2.62	2.29	2.22	2.16	2.16	1.61	1.51	1.48	1.47	1.47
Switch	0.00	0.84	0.70	0.32	0.31	0.30	0.30	0.30	0.27	0.27	0.26	0.26	0.26

Table II: RMS T-GOSPA Cost for All Trajectories

L -scan	T-IEMB-UKF					T-IEMB-IPLF				
	1	2	5	10	15	1	2	5	10	15
Total	7.75	7.36	7.16	7.09	7.09	5.94	5.49	5.29	5.31	5.31
Localisation	5.51	5.29	5.05	5.02	5.01	4.83	4.34	4.12	4.15	4.14
Missed	4.58	4.38	4.36	4.32	4.32	3.05	3.01	2.98	2.98	2.98
False	2.95	2.62	2.59	2.52	2.52	1.58	1.48	1.44	1.43	1.43
Switch	0.38	0.36	0.36	0.35	0.35	0.33	0.32	0.31	0.31	0.31

density where birth particles are spread across the surveillance area. This results in it generally taking many time steps to initialise a new target, while the birth densities for both GT-IEMB implementation generally allow for easier initialisation of trajectories.

The increase in missed and false target costs coinciding with target deaths, around time steps 57 and 64, is in fact a consequence of trajectory switching. That is, since we are estimating only alive trajectories, when a trajectory estimate switches the portion before the switch is then estimating a different ground truth trajectory, which may die before the one it has switched to. This results in a potential increase in missed and false target cost at some future point, as observed in Figure 5. Such behaviour would not be observed when estimating the set of all trajectories.

Table I contains the tabulated RMS T-GOSPA costs for all filters estimating the set of alive trajectories, which were generated using (82). The T-IEMB-IPLF is best performing, with T-IMB-IPLF worst performing. Both T-IMB implementation are affected by a high false target cost, as the IMB assumes target contributions do not overlap. When this assumption does not hold, false targets are subsequently initialised. Further illustrated is the reduction in cost by increasing the L -scan length for trajectory-based filters, where the performance difference between $L = 10$ and $L = 15$ is negligible. This implies that an L -scan length above 10 provides no further improvement, at least for the considered scenario.

Table II contains the tabulated RMS T-GOSPA costs for each GT-IEMB implementation for estimating the set of all trajectories. T-IEMB-IPLF is again the best performing filter, with increasing L -scan lengths also improving performance for each GT-IEMB implementation.

The average run time for a single MC was 271.3 s for the GPP-MB², 7.7 s for T-IMB-UKF, 67.4 s for T-IMB-IPLF, 1.6 s for T-IEMB-UKF, and 4.8 s for T-IEMB-IPLF. All filters were simulated on a laptop with a 2.4 GHz Intel i5 CPU and integrated Intel Iris Xe GPU. Each run time is quoted for an L -scan length of 1 for trajectory-based filters, where increasing the L -scan length has a negligible effect on run time.

²GPP-MB was simulated using a MATLAB/MEX implementation, meaning its run time is not directly comparable to the Python implementations.

Both GT-IEMB run times are low owing to their computationally light Gaussian filtering solution, and accurate estimation of the number of targets in the scenario. While the T-IMB is also a Gaussian filtering based solution, its very high false target cost increases its computational load as the filter initialises and updates a high number of trajectories. GPP-MB run time is highest, due to its particle filter based structure which is a computationally intensive approach.

VI. CONCLUSION

In this work we have extended the IEMB to estimate sets of trajectories from generalised superpositional measurements, which can be used to model non-Gaussian measurements. The T-IEMB recursion has been presented for estimating both the set of alive and all trajectories. A Gaussian implementation has been proposed, termed GT-IEMB, which performs the update using the conditional moments of the measurement. A Taylor series linearisation was proposed to form an approximation of the conditional moments of the generalised superpositional measurements.

Simulation results for a non-Gaussian multi-target tracking scenario have demonstrated the performance of two implementations of the GT-IEMB, one using the UKF and another using the IPLF. Both implementations outperformed the GPP-MB, which is a state-of-the-art particle filter for performing TkBD. Each implementation of the GT-IEMB also incurs a lower computational cost than the GPP-MB, owing to the computationally light structure of their Gaussian implementation compared to a particle filtering approach.

Future work includes the application of the developed GT-IEMB to challenging non-Gaussian tracking scenarios e.g. K-distributed sea clutter [33], and validation of the filters using real data. Implementation of the T-IEMB using SMC techniques is also another line of future work.

REFERENCES

- [1] S. Blackman and R. Popoli, *Design and Analysis of Modern Tracking Systems*. Artech House, 1999.
- [2] B. Ristic, L. Rosenberg, and D. Y. Kim, “Multi-Target Bernoulli Track-Before-Detect for OTHR,” *IEEE Transactions on Aerospace and Electronic Systems*, pp. 1–10, 2025.

- [3] P. Yang, D. Duan, C. Chen, X. Cheng, and L. Yang, "Multi-Sensor Multi-Vehicle (MSMV) Localization and Mobility Tracking for Autonomous Driving," *IEEE Transactions on Vehicular Technology*, vol. 69, no. 12, pp. 14 355–14 364, 2020.
- [4] E. Delande, J. Houssineau, J. Franco, C. Frueh, D. Clark, and M. Jah, "A new multi-target tracking algorithm for a large number of orbiting objects," *Advances in Space Research*, vol. 64, no. 3, pp. 645–667, 2019.
- [5] E. S. Davies and A. F. García-Fernández, "Information Exchange Track-Before-Detect Multi-Bernoulli Filter for Superpositional Sensors," *IEEE Transactions on Signal Processing*, vol. 72, pp. 607–621, 2024.
- [6] B. Ristic, D. Y. Kim, L. Rosenberg, and R. Guan, "Bernoulli Multi-Target Track-Before-Detect for Maritime Radar," in 2020 *IEEE International Radar Conference (RADAR)*, 2020, pp. 878–883.
- [7] D. Bossér, G. Hendeby, M. L. Nordenvaag, and I. Skog, "Broadband Passive Sonar Track-Before-Detect Using Raw Acoustic Data," *IEEE Journal of Oceanic Engineering*, vol. 50, no. 4, pp. 3106–3116, 2025.
- [8] M. Liang, T. Kropfreiter, and F. Meyer, "A BP Method for Track-Before-Detect," *IEEE Signal Processing Letters*, vol. 30, pp. 1137–1141, 2023.
- [9] H. Wu, Y. Cheng, X. Chen, Z. Yang, and X. Li, "Information Geometry-Based Track-Before-Detect Algorithm for Slow-Moving Fluctuating Target Detection," *IEEE Transactions on Signal Processing*, vol. 71, pp. 1833–1848, 2023.
- [10] W. Yi, Z. Fang, W. Li, R. Hoseinnezhad, and L. Kong, "Multi-Frame Track-Before-Detect Algorithm for Maneuvering Target Tracking," *IEEE Transactions on Vehicular Technology*, vol. 69, no. 4, pp. 4104–4118, 2020.
- [11] T. Kirubarajan and Y. Bar-Shalom, "Low Observable Target Motion Analysis Using Amplitude Information," in *IEE Colloquium on Algorithms for Target Tracking*, 1995, pp. 31–35.
- [12] D. Salmond and H. Birch, "A particle filter for track-before-detect," in *Proceedings of the 2001 American Control Conference. (Cat. No.01CH37148)*, vol. 5, 2001, pp. 3755–3760 vol.5.
- [13] R. Mahler, *Advances in Statistical Multisource-Multitarget Information Fusion*. Norwood, MA, USA: Artech House, 2014.
- [14] Á. F. García-Fernández, "Track-Before-Detect Labeled Multi-Bernoulli Particle Filter With Label Switching," *IEEE Transactions on Aerospace and Electronic Systems*, vol. 52, no. 5, pp. 2123–2138, 2016.
- [15] Á. F. García-Fernández, J. Grajal, and M. R. Morelande, "Two-layer particle filter for multiple target detection and tracking," *IEEE Transactions on Aerospace and Electronic Systems*, vol. 49, no. 3, pp. 1569–1588, 2013.
- [16] M. R. Morelande, C. M. Kreucher, and K. Kastella, "A Bayesian Approach to Multiple Target Detection and Tracking," *IEEE Transactions on Signal Processing*, vol. 55, no. 5, pp. 1589–1604, 2007.
- [17] F. Daum and J. Huang, "Curse of dimensionality and particle filters," in *2003 IEEE Aerospace Conference Proceedings (Cat. No.03TH8652)*, vol. 4, 2003, pp. 1979–1993.
- [18] S. Nannuru, M. Coates, and R. Mahler, "Computationally-Tractable Approximate PHD and CPHD Filters for Superpositional Sensors," *IEEE Journal of Selected Topics in Signal Processing*, vol. 7, no. 3, pp. 410–420, 2013.
- [19] S. Nannuru, Y. Li, Y. Zeng, M. Coates, and B. Yang, "Radio-Frequency Tomography for Passive Indoor Multitarget Tracking," *IEEE Transactions on Mobile Computing*, vol. 12, no. 12, pp. 2322–2333, 2013.
- [20] J. P. Beaudeau, M. F. Bugallo, and P. M. Djurić, "RSSI-Based Multi-Target Tracking by Cooperative Agents Using Fusion of Cross-Target Information," *IEEE Transactions on Signal Processing*, vol. 63, no. 19, pp. 5033–5044, 2015.
- [21] D. Hauschildt, "Gaussian mixture implementation of the cardinalized probability hypothesis density filter for superpositional sensors," in *2011 International Conference on Indoor Positioning and Indoor Navigation*, 2011, pp. 1–8.
- [22] S. Nannuru and M. Coates, "Multi-Bernoulli filter for superpositional sensors," in *Proceedings of the 16th International Conference on Information Fusion*, 2013, pp. 1632–1637.
- [23] —, "Particle filter implementation of the multi-Bernoulli filter for superpositional sensors," in *2013 5th IEEE International Workshop on Computational Advances in Multi-Sensor Adaptive Processing (CAMSAP)*, 2013, pp. 368–371.
- [24] C. M. Bishop, *Pattern Recognition and Machine Learning*. New York, NY, USA: Springer Science + Business Media, 2006.
- [25] P. M. Djuric, T. Lu, and M. F. Bugallo, "Multiple Particle Filtering," in *2007 IEEE International Conference on Acoustics, Speech and Signal Processing - ICASSP '07*, vol. 3, 2007, pp. III-1181–III-1184.
- [26] P. Closas, C. Fernandez-Prades, and J. Vila-Valls, "Multiple Quadrature Kalman Filtering," *IEEE Transactions on Signal Processing*, vol. 60, no. 12, pp. 6125–6137, 2012.
- [27] Á. F. García-Fernández, L. Svensson, and M. R. Morelande, "Multiple Target Tracking Based on Sets of Trajectories," *IEEE Transactions on Aerospace and Electronic Systems*, vol. 56, no. 3, pp. 1685–1707, 2020.
- [28] Á. F. García-Fernández, L. Svensson, J. L. Williams, Y. Xia, and K. Granström, "Trajectory multi-Bernoulli filters for multi-target tracking based on sets of trajectories," in *2020 IEEE 23rd International Conference on Information Fusion (FUSION)*, 2020, pp. 1–8.
- [29] —, "Trajectory Poisson Multi-Bernoulli Filters," *IEEE Transactions on Signal Processing*, vol. 68, pp. 4933–4945, 2020.
- [30] Á. F. García-Fernández and L. Svensson, "Trajectory PHD and CPHD Filters," *IEEE Transactions on Signal Processing*, vol. 67, no. 22, pp. 5702–5714, 2019.
- [31] F. Tronarp, Á. F. García-Fernández, and S. Särkkä, "Iterative Filtering and Smoothing in Nonlinear and Non-Gaussian Systems Using Conditional Moments," *IEEE Signal Processing Letters*, vol. 25, no. 3, pp. 408–412, 2018.
- [32] M. Mallick, V. Krishnamurthy, and B.-N. Vo, *Integrated Tracking, Classification, and Sensor Management: Theory and Applications*. Hoboken, NJ, USA: Wiley, 2013.
- [33] K. Ward, R. Tough, and S. Watts, *Sea Clutter: Scattering, the K Distribution and Radar Performance*, 2nd ed. The Institution of Engineering and Technology, 2013.
- [34] Á. F. García-Fernández, L. Svensson, M. R. Morelande, and S. Särkkä, "Posterior Linearization Filter: Principles and Implementation Using Sigma Points," *IEEE Transactions on Signal Processing*, vol. 63, no. 20, pp. 5561–5573, 2015.
- [35] S. Lynch, Á. F. García-Fernández, and L. Devlin, "Trajectory Information Exchange Multi-Bernoulli Filtering for Track-Before-Detect," in *2025 28th International Conference on Information Fusion (FUSION)*, 2025, pp. 1–8.
- [36] M. A. Richards, J. Scheer, and W. A. Holm, *Principles of Modern Radar: Volume I, Basic principles*. Raleigh, NC: SciTech Pub., 2010.
- [37] A. Papoulis and S. U. Pillai, *Probability, Random Variables and Stochastic Processes*. New York, NY: McGraw-Hill, 2002.
- [38] K. Granström, L. Svensson, Y. Xia, J. Williams, and Á. F. García-Fernández, "Poisson Multi-Bernoulli Mixtures for Sets of Trajectories," *IEEE Transactions on Aerospace and Electronic Systems*, vol. 61, no. 2, pp. 5178–5194, 2025.
- [39] I. Arasaratnam, S. Haykin, and R. J. Elliott, "Discrete-Time Nonlinear Filtering Algorithms Using Gauss-Hermite Quadrature," *Proceedings of the IEEE*, vol. 95, no. 5, pp. 953–977, 2007.
- [40] Á. F. García-Fernández, F. Tronarp, and S. Särkkä, "Gaussian Target Tracking With Direction-of-Arrival von Mises-Fisher Measurements," *IEEE Transactions on Signal Processing*, vol. 67, no. 11, pp. 2960–2972, 2019.
- [41] S. Särkkä, *Bayesian Filtering and Smoothing*, 2nd ed. Cambridge, UK: Cambridge University Press, 2023.
- [42] Á. F. García-Fernández, S. Maskell, P. Horridge, and J. Ralph, "Gaussian Tracking With Kent-Distributed Direction-of-Arrival Measurements," *IEEE Transactions on Vehicular Technology*, vol. 70, no. 7, pp. 7249–7254, 2021.
- [43] F. Beutler, M. F. Huber, and U. D. Hanebeck, "Gaussian Filtering using state decomposition methods," in *2009 12th International Conference on Information Fusion*, 2009, pp. 579–586.
- [44] Á. F. García-Fernández, J. Ralph, P. Horridge, and S. Maskell, "Gaussian trajectory PMBM filter with nonlinear measurements based on posterior linearisation," in *2022 25th International Conference on Information Fusion (FUSION)*, 2022, pp. 01–08.
- [45] Y. Bar-Shalom, X. Li, and T. Kirubarajan, *Estimation with Applications to Tracking and Navigation*. Hoboken, NJ, USA: Wiley, 2001.
- [46] J. H. Park, "Moments of the Generalized Rayleigh Distribution," *Quarterly of Applied Mathematics*, vol. 19, no. 1, pp. 45–49, 1961.
- [47] M. Abramowitz and I. A. Stegun, *Handbook of Mathematical Functions With Formulas, Graphs and Mathematical Tables*, 10th ed., ser. Applied Mathematics Series. Washington D.C.: National Bureau of Standards, 1972.
- [48] B.-N. Vo, B.-T. Vo, N.-T. Pham, and D. Suter, "Joint Detection and Estimation of Multiple Objects From Image Observations," *IEEE Transactions on Signal Processing*, vol. 58, no. 10, pp. 5129–5141, 2010.
- [49] Á. F. García-Fernández, A. S. Rahmathullah, and L. Svensson, "A Metric on the Space of Finite Sets of Trajectories for Evaluation of Multi-Target Tracking Algorithms," *IEEE Transactions on Signal Processing*, vol. 68, pp. 3917–3928, 2020.

A Track-Before-Detect Trajectory Multi-Bernoulli Filter for Generalised Superpositional Measurements: Supplemental Material

APPENDIX A

This appendix reviews integration for functions on sets of trajectories.

Given some real valued function $\pi(\cdot)$ on the single-trajectory space $T_{(k)}$, its integral is given by [27]

$$\int \pi(X) dX = \sum_{(t,v) \in I_{(k)}} \int \pi(t, x^{1:v}) dx^{1:v} \quad (83)$$

where the summation goes through all possible start times, lengths and target states. Given a real valued function $\pi(\cdot)$ on the space of sets of trajectories $\mathcal{F}(T_{(k)})$, the set integral is

$$\int \pi(\mathbf{X}) d\mathbf{X} = \sum_{n=0}^{\infty} \frac{1}{n!} \int \pi(\{X_1, \dots, X_n\}) dX_{1:n}. \quad (84)$$

APPENDIX B

This appendix derives the update for the set of all trajectories in Lemma 4.

Given the single-trajectory density form (21), the posterior density for all trajectories is found by taking the predicted Bernoulli of the form (25) and plugging into the update (27), which yields

$$\tilde{f}_{k|k}^u(\tilde{\mathbf{X}}_k) \propto \begin{cases} r_{k|k-1}^u \vartheta(X) & \tilde{\mathbf{X}}_k = \{(u, X)\} \\ p^u(z_k|\emptyset)(1 - r_{k|k-1}^u) & \tilde{\mathbf{X}}_k = \emptyset \\ 0 & \text{otherwise} \end{cases} \quad (85)$$

where

$$\begin{aligned} \vartheta(X) &= p^u(z_k|\tau^k(X)) \beta_{k|k-1}^u(k) p_{k|k-1}^{u,k}(X) \\ &\quad + p^u(z_k|\emptyset) \sum_{l=t^u}^{k-1} \beta_{k|k-1}^u(l) p_{k|k-1}^{u,l}(X). \end{aligned} \quad (86)$$

Let us simplify $\vartheta(X)$ as

$$\begin{aligned} \vartheta(X) &= \beta_{k|k-1}^u(k) \left[\int p^u(z_k|\tau^k(X)) p_{k|k-1}^{u,k}(X) dX \right] \\ &\quad \times \frac{p^u(z_k|\tau^k(X)) p_{k|k-1}^{u,k}(X)}{\int p^u(z_k|\tau^k(X)) p_{k|k-1}^{u,k}(X) dX} \\ &\quad + p^u(z_k|\emptyset) \sum_{l=t^u}^{k-1} \beta_{k|k-1}^u(l) p_{k|k-1}^{u,l}(X) \\ &= \beta_{k|k-1}^u(k) p^u(z_k||\tilde{\mathbf{x}}_k| = 1) p_{k|k}^{u,k}(X) \\ &\quad + p^u(z_k|\emptyset) \sum_{l=t^u}^{k-1} \beta_{k|k-1}^u(l) p_{k|k-1}^{u,l}(X) \end{aligned} \quad (87)$$

where

$$p^u(z_k||\tilde{\mathbf{x}}_k| = 1) = \int p^u(z_k|\tau^k(X)) p_{k|k-1}^{u,k}(X) dX \quad (88)$$

$$p_{k|k}^{u,l}(X) = \begin{cases} p_{k|k-1}^{u,l}(X) & l \in \{t^u, \dots, k-1\} \\ \frac{p^u(z_k|\tau^k(X)) p_{k|k-1}^{u,k}(X)}{\int p^u(z_k|\tau^k(X)) p_{k|k-1}^{u,k}(X) dX} & l = k. \end{cases} \quad (89)$$

We now factorise (87) as

$$\begin{aligned} \vartheta(X) &= \rho_k^u \left[\frac{\beta_{k|k-1}^u(k) p^u(z_k||\tilde{\mathbf{x}}_k| = 1)}{\rho_k^u} p_{k|k}^{u,k}(X) \right] \\ &\quad + \rho_k^u \left[p^u(z_k|\emptyset) \sum_{l=t^u}^{k-1} \frac{\beta_{k|k-1}^u(l)}{\rho_k^u} p_{k|k}^{u,l}(X) \right] \end{aligned} \quad (90)$$

where

$$\rho_k^u = \beta_{k|k-1}^u(k) p^u(z_k||\tilde{\mathbf{x}}_k| = 1) + p^u(z_k|\emptyset) \sum_{l=t^u}^{k-1} \beta_{k|k-1}^u(l). \quad (91)$$

Considering $\vartheta(X)$ as (90), this implies that the updated existence probability and Beta parameters are

$$r_{k|k}^u = \frac{\rho_k^u r_{k|k-1}^u}{\rho_k^u r_{k|k-1}^u + p^u(z_k|\emptyset)(1 - r_{k|k-1}^u)} \quad (92)$$

$$\beta_{k|k}^u(l) \propto \begin{cases} p^u(z_k|\emptyset) \beta_{k|k-1}^u(l) & l \in \{t^u, \dots, k-1\} \\ p^u(z_k||\tilde{\mathbf{x}}_k| = 1) \beta_{k|k-1}^u(k) & l = k. \end{cases} \quad (93)$$

The updated single-trajectory densities are given by (89), which finishes the proof of Lemma 4.

APPENDIX C

This appendix includes the prediction stage of the GT-IEMB for alive and all trajectories.

Gaussian Densities: We assume that target states evolve according to a linear-Gaussian transition density $g(\cdot|x_{k-1}) = \mathcal{N}(\cdot; Fx_{k-1}, Q)$, where F is the state transition matrix, and Q is the process noise covariance matrix. Existing targets survive to the next time step with a constant probability of survival $p^S(x) = p^S$, and new targets are born according to the MB birth model (12) with Gaussian single-target birth densities \bar{x}_b^l and P_b^l .

GT-IEMB Prediction for Alive Trajectories: Given a TMB density of the form (16) at time step $k-1$, the prediction for the GT-IEMB is given by [29]

$$\bar{F}_i = [0_{1,\iota-1}, 1] \otimes F \quad (94)$$

$$\bar{x}_{k|k-1}^i = \left[(\bar{x}_{k-1|k-1}^i)^T, (\bar{F}_i \bar{x}_{k-1|k-1}^i)^T \right]^T \quad (95)$$

$$P_{k|k-1}^i = \begin{bmatrix} P_{k-1|k-1}^i & P_{k-1|k-1}^i \bar{F}_i^T \\ \bar{F}_i P_{k-1|k-1}^i & \bar{F}_i P_{k-1|k-1}^i \bar{F}_i^T + Q \end{bmatrix} \quad (96)$$

$$r_{k|k-1}^i = p^S r_{k-1|k-1}^i \quad (97)$$

where $0_{n,m}$ is an $n \times m$ matrix of zeros, and \otimes denotes the Kronecker product. We also introduce birth components in the prediction stage, from the Bernoulli birth model defined in Section III-A. The mean, covariance and birth probabilities for each birth component is

$$\bar{x}_{k|k-1}^i = \bar{x}_b^{i-n_{k-1|k-1}}, P_{k|k-1}^i = P_b^{i-n_{k-1|k-1}}$$

$$r_{k|k-1}^i = p_b^{i-n_{k-1|k-1}} \quad (98)$$

where $i \in \{n_{k-1|k-1} + 1, \dots, n_{k-1|k-1} + n_k^b\}$.

GT-IEMB Prediction for All Trajectories: Given a TMB density of the form (16) at time step $k-1$, we obtain the predicted trajectory mean and covariance of each Bernoulli component using the same prediction presented in (94)–(97) for $\bar{x}_{k-1|k-1}^i(l)$ and $P_{k-1|k-1}^i(l)$, where $l = k$. For $l \in \{t^i, \dots, k-1\}$ we do not perform a prediction, meaning $\bar{x}_{k|k-1}^i(l) = \bar{x}_{k-1|k-1}^i(l)$ and $P_{k|k-1}^i(l) = P_{k-1|k-1}^i(l)$. The predicted existence probability is given by $r_{k|k-1}^i = r_{k-1|k-1}^i$, and we also introduce the birth components (98).

For the set of all trajectories, we must also consider $\beta_{k|k-1}^i(l)$, which is predicted using [29]

$$\beta_{k|k-1}^i(l) = \begin{cases} \beta_{k-1|k-1}^i(l) & l \in \{t^i, \dots, k-2\} \\ (1-p^S)\beta_{k-1|k-1}^i(l) & l = k-1 \\ p^S\beta_{k-1|k-1}^i(l) & l = k \end{cases} \quad (99)$$

where we account for the hypothesis that the trajectory terminates at the current time step $p^S\beta_{k-1|k-1}^i(l)$, and the hypothesis that it terminated at the previous time step $(1-p^S)\beta_{k-1|k-1}^i(l)$. We clarify that while the mean and covariance $\bar{x}_{k|k-1}^i(l)$ and $P_{k|k-1}^i(l)$ for $l = k-1$ are unchanged in the prediction stage, there is a change to $\beta_{k|k-1}^i(l)$ for $l = k-1$ to account for the probability that the trajectory died at this time step.

APPENDIX D

This appendix provides the proof of Lemma 5. That is, we prove the mean and covariance of h^i , and the mean of R^i , which are presented in (44), 6 and (46), respectively.

The density of h^i is

$$\begin{aligned} p_{k|k-1}^i(h^i) &= \int \tilde{f}_{k|k-1}^i(\tilde{\mathbf{x}}_k^i, h^i) \delta \tilde{\mathbf{x}}_k^i \\ &= (1 - r_{k|k-1}^i(k)) \delta_0(h^i) \\ &+ r_{k|k-1}^i(k) \int \delta_{h(x)}(h^i) p_{k|k-1}^i(x) dx \end{aligned} \quad (100)$$

where the mean is then given by

$$\begin{aligned} \mathbb{E}[h^i] &= (1 - r_{k|k-1}^i(k))0 + r_{k|k-1}^i(k) \mathbb{E}_i[h(x)] \\ &= r_{k|k-1}^i(k) \mathbb{E}_i[h(x)] \end{aligned} \quad (101)$$

and the covariance

$$\begin{aligned} \mathbb{C}[h^i] &= \mathbb{E}[\mathbb{C}[h^i|\tilde{\mathbf{x}}_k^i]] + \mathbb{C}[\mathbb{E}[h^i|\tilde{\mathbf{x}}_k^i]] \\ &= 0 + \mathbb{E}[\mathbb{E}[h^i|\tilde{\mathbf{x}}_k^i] \mathbb{E}[h^i|\tilde{\mathbf{x}}_k^i]^T] - \mathbb{E}[h^i] \mathbb{E}[h^i]^T \end{aligned} \quad (102)$$

where

$$\begin{aligned} \mathbb{E}[\mathbb{E}[h^i|\tilde{\mathbf{x}}_k^i] \mathbb{E}[h^i|\tilde{\mathbf{x}}_k^i]^T] &= (1 - r_{k|k-1}^i(k)) \mathbb{E}[h^i|\emptyset] \mathbb{E}[h^i|\emptyset]^T + \\ &+ r_{k|k-1}^i(k) \int h(x)(h(x))^T p_{k|k-1}^i(x) dx \\ &= r_{k|k-1}^i(k) \int h(x)(h(x))^T p_{k|k-1}^i(x) dx. \end{aligned} \quad (103)$$

Therefore, the covariance of h^i is given by

$$\begin{aligned} \mathbb{C}[h^i] &= r_{k|k-1}^i(k) \int h(x)(h(x))^T p_{k|k-1}^i(x) dx \\ &- (r_{k|k-1}^i(k))^2 \mathbb{E}_i[h(x)] \mathbb{E}_i[h(x)]^T \end{aligned} \quad (104)$$

The mean of R^i is derived analogously to the mean of h^i .

APPENDIX E

This appendix proves Proposition 7. That is, it provides the proof for the conditional mean and covariance of the measurement, presented in (57) and (58), following the notation of Section IV-B.

The mean of the measurement conditioned on $\tilde{\mathbf{x}}_k^u = \{(u, x^u)\}$ is given by

$$\begin{aligned} \mathbb{E}[z_k|\tilde{\mathbf{x}}_k^u = \{(u, x^u)\}] &= \int \mathbb{E}[z_k|\{(u, x^u)\} \cup \tilde{\mathbf{x}}_k^{(-u)}] \\ &\times \prod_{i=1:i \neq u}^{n_{k|k-1}} \tilde{f}_{k|k-1}^i(\tilde{\mathbf{x}}_k^i) \delta \tilde{\mathbf{x}}_k^{(-u)} \\ &= \int m(h(x^u) + h^{(-u)}) \\ &\times \prod_{i=1:i \neq u}^{n_{k|k-1}} \tilde{f}_{k|k-1}^i(\tilde{\mathbf{x}}_k^i) \delta \tilde{\mathbf{x}}_k^{(-u)} \end{aligned} \quad (105)$$

where we have used the result of (5) and (50). Applying the change of variables formula for set integrals [13, Sec. 3.5.2] yields

$$\begin{aligned} \mathbb{E}[z_k|\tilde{\mathbf{x}}_k^u = \{(u, x^u)\}] &= \int m(h(x^u) + h^{(-u)}) \\ &\times p(h^{(-u)}) dh^{(-u)} \end{aligned} \quad (106)$$

where $p(h^{(-u)})$ is the density of $h^{(-u)}$, whose mean \hat{h}_{corr}^u and covariance S_{corr}^u are given in Lemma 6. Applying the Taylor series approximation (55) we obtain

$$\begin{aligned} \mathbb{E}[z_k|\tilde{\mathbf{x}}_k^u = \{(u, x^u)\}] &\approx \\ &\int [m(h(x^u) + \hat{h}_{corr}^u) + M(h(x^u) + \hat{h}_{corr}^u)(h^{(-u)} - \hat{h}_{corr}^u)] \\ &\times p(h^{(-u)}) dh^{(-u)} \\ &= m(h(x^u) + \hat{h}_{corr}^u) \int p(h^{(-u)}) dh^{(-u)} \\ &+ M(h(x^u) + \hat{h}_{corr}^u) \int (h^{(-u)} - \hat{h}_{corr}^u) p(h^{(-u)}) dh^{(-u)} \\ &= m(h(x^u) + \hat{h}_{corr}^u) \end{aligned} \quad (107)$$

since $\int h^{(-u)} p(h^{(-u)}) dh^{(-u)} = \hat{h}_{corr}^u$.

The covariance of the measurement conditioned on $\tilde{\mathbf{x}}_k^u = \{(u, x^u)\}$ can be written using the law of total covariance as

$$\begin{aligned} \mathbb{C}[z_k|\tilde{\mathbf{x}}_k^u = \{(u, x^u)\}] &= \int \mathbb{C}[z_k|\{(u, x^u)\} \cup \tilde{\mathbf{x}}_k^{(-u)}] \times \prod_{i=1:i \neq u}^{n_{k|k-1}} \tilde{f}_{k|k-1}^i(\tilde{\mathbf{x}}_k^i) \delta \tilde{\mathbf{x}}_k^{(-u)} \\ &+ \mathbb{C}[\mathbb{E}[z_k|\tilde{\mathbf{x}}_k^u = \{(u, x^u)\} \cup \tilde{\mathbf{x}}_k^{(-u)}] | \tilde{\mathbf{x}}_k^u = \{(u, x^u)\}] \end{aligned} \quad (108)$$

Using (6) and (51), the first term can be written as

$$\begin{aligned} & \int C \left[z_k | \{(u, x^u)\} \cup \tilde{\mathbf{x}}_k^{(-u)} \right] \times \prod_{i=1: i \neq u}^{n_{k|k-1}} \tilde{f}_{k|k-1}^i(\tilde{\mathbf{x}}_k^i) \delta \tilde{\mathbf{x}}_k^{(-u)} \\ &= \int \Sigma(R(x^u) + R^{(-u)}) \times \prod_{i=1: i \neq u}^{n_{k|k-1}} \tilde{f}_{k|k-1}^i(\tilde{\mathbf{x}}_k^i) \delta \tilde{\mathbf{x}}_k^{(-u)} \end{aligned} \quad (109)$$

and can be approximated using the zero-order Taylor series approximation (56), which gives

$$\begin{aligned} & \int \Sigma(R(x^u) + R^{(-u)}) \times \prod_{i=1: i \neq u}^{n_{k|k-1}} \tilde{f}_{k|k-1}^i(\tilde{\mathbf{x}}_k^i) \delta \tilde{\mathbf{x}}_k^{(-u)} \\ & \approx \int \Sigma(R(x^u) + R_{corr}^u) \times \prod_{i=1: i \neq u}^{n_{k|k-1}} \tilde{f}_{k|k-1}^i(\tilde{\mathbf{x}}_k^i) \delta \tilde{\mathbf{x}}_k^{(-u)} \\ &= \Sigma(R(x^u) + R_{corr}^u). \end{aligned} \quad (110)$$

The second term can then be written using (5) as

$$\begin{aligned} & C \left[E \left[z_k | \tilde{\mathbf{x}}_k^u = \{(u, x^u)\} \cup \tilde{\mathbf{x}}_k^{(-u)} \right] | \tilde{\mathbf{x}}_k^u = \{(u, x^u)\} \right] \\ &= C \left[m(h(x^u) + h^{(-u)}) | \tilde{\mathbf{x}}_k^u = \{(u, x^u)\} \right] \end{aligned} \quad (111)$$

where we can approximate $m(h(x^u) + h^{(-u)})$ using (55), and this result gives

$$\begin{aligned} & C \left[m(h(x^u) + h^{(-u)}) | \tilde{\mathbf{x}}_k^u = \{(u, x^u)\} \right] \\ &= C \left[M(h(x^u) + \hat{h}_{corr}^u)(h^{(-u)} - \hat{h}_{corr}^u) | \tilde{\mathbf{x}}_k^u = \{(u, x^u)\} \right] \\ &= M(h(x^u) + \hat{h}_{corr}^u) S_{corr}^u M(h(x^u) + \hat{h}_{corr}^u)^T \end{aligned} \quad (112)$$

where $m(h(x^u) + \hat{h}_{corr}^u)$ is omitted as its covariance with respect to $\tilde{\mathbf{x}}_k^u$ is 0.

For the case where $\tilde{\mathbf{x}}_k^u = \emptyset$, the conditional mean is now approximated by

$$m(h^{(-u)}) \approx m(\hat{h}_{corr}^u). \quad (113)$$

For the conditional covariance, the first term in (108) reduces to

$$\int C \left[z_k | \tilde{\mathbf{x}}_k^{(-u)} \right] \times \prod_{i=1: i \neq u}^{n_{k|k-1}} \tilde{f}_{k|k-1}^i(\tilde{\mathbf{x}}_k^i) \delta \tilde{\mathbf{x}}_k^{(-u)} \approx \Sigma(R_{corr}^u) \quad (114)$$

and the second term, using the expansion

$$m(h^{(-u)}) \approx m(\hat{h}_{corr}^u) + M(\hat{h}_{corr}^u)(h^{(-u)} - \hat{h}_{corr}^u) \quad (115)$$

reduces to

$$\begin{aligned} & C \left[m(h^{(-u)}) | \tilde{\mathbf{x}}_k^u = \{(u, x^u)\} \right] \\ &= C \left[M(\hat{h}_{corr}^u)(h^{(-u)} - \hat{h}_{corr}^u) | \tilde{\mathbf{x}}_k^u = \{(u, x^u)\} \right] \\ &= M(\hat{h}_{corr}^u) S_{corr}^u M(\hat{h}_{corr}^u) \end{aligned} \quad (116)$$

where we have used a Taylor series expansion of $m(h^{(-u)})$ around \hat{h}_{corr}^u .

APPENDIX F

This appendix details the approach used to update past trajectory information using the current time step updated moments.

Performing the prediction stage produces a predicted single-trajectory density, which we can view considering the current time step k and all previous time steps. Following the notation in [44], we denote the predicted mean and covariance for the current time step as $\bar{x} = \mu_{k|k-1}^i$ and $P_{xx} = \Xi_{k|k-1}^i$, respectively, and the predicted cross covariance is denoted P_{xy} . All previous time steps have trajectory mean $\bar{y} = \bar{x}_{k|k-1}^i(k-1)$ and covariance $P_{yy} = P_{k|k-1}^i(k-1)$.

This density is Gaussian and can be written as

$$p(y, x) = \mathcal{N} \left([y^T, x^T]^T; [\bar{y}^T, \bar{x}^T]^T, \begin{bmatrix} P_{yy} & P_{xy}^T \\ P_{xy} & P_{xx} \end{bmatrix} \right). \quad (117)$$

The single-target IEMB update in Section IV-C computes the updated target mean and covariance for the current time step, which we denote $\bar{u}_x = \mu_{k|k}^i$ and $W_{xx} = \Xi_{k|k}^i$, respectively. Both are used to calculate the updated single-trajectory density mean \bar{u} and covariance W , which are given by [43]

$$\bar{u} = [\bar{u}_y^T, \bar{u}_x^T]^T, W = \begin{bmatrix} W_{yy} & W_{xy}^T \\ W_{xy} & W_{xx} \end{bmatrix} \quad (118)$$

where

$$\bar{u}_y = \bar{y} + G(\bar{u}_x - \bar{x}) \quad (119)$$

$$W_{xy} = W_{xx} G^T \quad (120)$$

$$W_{yy} = P_{yy} - G(P_{xx} - W_{xx})G^T \quad (121)$$

$$G = P_{xy}^T P_{xx}^{-1}. \quad (122)$$

For the updated trajectory mean, \bar{u}_y corresponds to previous trajectory states which are updated using the updated single-target density. Under the L -scan approximation, this is the $L-1$ most recent time steps. Trajectory states before \bar{u}_y remain unchanged, as they are outside the L -scan window. The covariance matrix W is also bound to size $L n_x \times L n_x$, which then contains the covariance across the L most recent time steps.

APPENDIX G

This appendix provides some useful results regarding the moments of the Rician distributed measurements.

For the conditional measurement mean in (79), we note that [47, 22.5.54]

$$L_{1/2}(x) = L_{1/2}^{(0)}(x) = M \left(-\frac{1}{2}, 1, x \right) \quad (123)$$

where $L_{1/2}^{(0)}(x)$ is the generalised Laguerre polynomial, and $M(-\frac{1}{2}, 1, x)$ denotes the confluent hypergeometric function of the first kind (Kummer's function) [47, Chapter 13]. To form the conditional measurement covariance in (58), we require the Jacobian of $m(\cdot)$, which involves partial differentiation of $m(\cdot)$. We note that the following result proves useful [47, 13.4.8]

$$\frac{\partial}{\partial x} M(a, b, x) = \frac{a}{b} M(a+1, b+1, x). \quad (124)$$